Journal of Computational Applied Mechanics 2024, 55(-): PP-PP

DOI: 10.22059/JCAMECH.2024.374402.1022

RESEARCH PAPER

Estimation of Elastic and Piezoelectric Properties of Short Piezo Fuzzy Fiber Reinforced Composite Using Method of Cells Micromechanics Approach

Rahul Sharma, Rajana Suresh Kumar *

Department of Mechanical Engineering, NIT Raipur, Raipur 492001, India

Abstract

Piezoelectric fibers are being widely used in the development of devices such as sensors, actuators, energy harvesting equipment, and in instruments related to biomedical engineering. Piezoelectric (PZT) fibers with radially grown carbon nanotubes (CNTs) on their surface when used as homogenous fiber in the preparation of a composite lamina is found to exhibit some enhanced elastic and piezo electric properties. The short piezoelectric fibers with radially grown CNTs which is known as piezo fuzzy fiber (PFF) are horizontally embedded in the polymer matrix to form short piezo fuzzy fiber reinforced composite (SPFFRC) lamina and the characterized mechanical properties estimated by method of cells (MOC) approach and the same has been compared with the conventional Mori-Tanaka (MT) method. The effect of waviness which are inherent to the CNTs on the overall properties have been estimated and are reported in the present study. Also, the significance of CNT orientation on the final elastic and piezo electric properties of SPFFRCs have been displayed in detail in the present study. The orientation of CNTs is vital and the results of the study show that when the CNTs are oriented transverse to the base fiber direction, the elastic properties are enhanced while the piezoelectric properties showed no or negligible effect on the orientation of CNTs. Also, the straight CNTs showed better performance in electric properties of SPFFRC while the performance slightly reduced with increase in waviness of CNTs. However, the effective elastic properties showed an increasing trend with increase in CNT waviness and hence, for the better use of the proposed SPFFRC as materials for actuator or sensor, the SPFFRC with wavy CNTs may be preferred since the waviness is inherent characteristic of CNTs and the waviness of CNTs has minimal effect on piezoelectric properties but has significant effect on the elastic properties.

* Corresponding author. Tel.: +91-9111244643
E-mail address: rskumar.me@nitrr.ac.in

Keywords: Piezoelectric Fiber (PZT); Carbon Nano Tubes (CNTs); Method of Cells (MOC); Mori-Tanaka (MT); Micromechanical Analysis; Piezo fuzzy fiber (PFF); Short Piezo Fuzzy Fiber Reinforced Composite (SPFFRC).

1. Introduction

The use of piezoelectric composites (PZCs) as actuators materials for smart structures is proven beyond doubt due to their superior material characteristics compared to monolithic piezoelectric materials [1-3]. Among the available PZCs, the lamina of vertically reinforced 1–3 PZC is widely used as the material of the actuators [4]. In the quest for better actuation, Mallik and Ray proposed piezoelectric fiber reinforced composite (PFRC) material having the piezoelectric fibers longitudinally reinforced in the epoxy matrix material [5]. They predicted that the effective piezoelectric co-efficient e_{31} of this PFRC material which quantifies the induced normal stress in the fiber direction due to the unit electric field applied transverse to the fiber direction is significantly larger than the corresponding co-efficient of the piezoelectric material of the fibers. Hence, the PFRCs prove to be effective actuator materials than that of the commercially available 1-3 PZCs. Ever since the discovery of the carbon nanotubes (CNTs) by Iijima [6], researchers have been exploring their potentiality of using these CNTs of various geometries along with the base fibers of the regular composite lamina seems to have exhibited remarkable enhancement in the overall mechanical properties of the composites. A single-walled CNT is a graphene sheet rolled in the form of tube [6]. These CNTs were found to have excellent elastic modulus in the axial direction in the range close to tera pascals [7]. Shen and Li [8] observed the transverse isotropy nature of the CNTs when the axis of isotropy coincides with the geometric centroidal axis of CNTs. Cheng et al., [9] estimated the mechanical properties of single walled CNTs by proposing an atomistic based continuum model. Because of exceptional elastic properties of CNT, a wide variety of CNT-reinforced composites can be manufactured and the properties can be estimated using different models like the micromechanical models and the atomistic continuum models. Thostenson and Chou [10] found the elastic properties of CNT reinforced composite using the micromechanics approach while Griebel and Hamaekers [11] estimated the same employing the molecular dynamics simulation. Employing the homogenous based continuum model, Odegard et al. [12] obtained the elastic moduli of CNT-reinforced composites while Seidel and Lagoudas [13] calculated the same using the Self consistent and Mori–Tanaka methods. Song and Youn [14] found numerically the effective elastic properties of CNT-reinforced composites. Jiang et al. [15] obtained the effective elastic properties of CNT-reinforced composites by maximizing the volume fraction of the CNT reinforcements. Ayatollahi et al. [16] presented the mechanical behavior of the CNT reinforced composites through multiscale modelling and obtained the properties of the same by analyzing them under tensile, bending and torsional loading conditions. They reported that the CNT reinforcements have caused a significant improvement in the mechanical properties. The inherent characteristics of the nanotubes owes to its waviness and the effect of this waviness on composite elastic properties has been analyzed and studied in detail by Fisher et al. [17]. The authors used a combined approach of finite element (FE) and the micromechanical analysis to estimate the elastic properties and showed that waviness plays a vital role when these tubes are used as reinforcements. The above studies pertaining to the use of CNTs as reinforcements in the composites have proven to be very effective and hence, the researchers came up with the idea of harnessing the potential of these CNTs in the development of newer materials. One such work towards the same led to the development of hybrid piezoelectric composite Ray and Batra [18] with CNTs vertically aligned and parallel to vertical piezo fibers. They found that the vertically aligned CNTs have indeed improved the effective properties of the proposed hybrid piezoelectric composite [18]. The methods for the growth of aligned CNTs on base composite substrates has been achieved using the chemical vapour deposition technique by Bower et al. [19] who were able to grow the nanotubes transverse to the direction of the substrate regardless of the size and shape of the substrate. Lanzara and Chang [20] came up with the technique to grow CNTs on the piezoelectric surface and achieved the bond strength between the actuator and substrate. Mathur et al. [21] experimentally found that the CNTs grown on the carbon fibers if the composite showed exceptional moduli and bending strength. Taking the method of growing the CNTs on the composite forward, researchers have produced variety of composites by growing the CNTs on different substrates like the aluminium silicate, quartz fiber, woven cloth of aluminium fiber and demonstrated that the properties of such composites have been greatly enhanced[22-26]. The earlier works were focused on using the CNTs as reinforcements on the substrate composites however, the work on augmentation of CNTs on long unidirectional fibers and their use in the composite lamina have also been found to influence their effective properties. Such fibers with radially grown CNTs on the periphery are termed as “fuzzy fiber” [21, 22] and the composite made from reinforcing this fuzzy fiber in the conventional epoxy matrix is called the “fuzzy fiber reinforced composite” (FFRC) [27]. The micromechanical analysis of these composite modelling has been proven

very effective and the results obtained are in good agreement with that of the experimental ones found in the literature. Hence, Kundalwal and his team in series of their works has used the micromechanics approaches like method of cells (MOC), mechanics of materials (MOM), effective medium (EM), and the Mori-Tanaka methods for estimating the thermomechanical properties FFRCs [27-31]. Recently, Alian et al., [26] and Kundalwal and Ray [27-30] derived micromechanics models for estimating all the effective elastic coefficients of fuzzy fiber-reinforced composite (FFRC). Mohammadi and his team in a series of works have reported the effect in-plane, shear, and the buckling effects on graphene plates and shells [32-36]. Also, his team carried out an extensive study on the vibration behavior of graphene-based structures [32-36]. Later, Arani and his team of co researchers studied the size dependent behavior of double bonded carbon nanotubes reinforced composite microtubes [37]. Arani et al., [38] studied the electro-magnetic wave propagation analysis of viscoelastic sandwich nanoplates under the influence of surface effects. Arani et al., [39] studied the nonlocal effects on the vibrations of piezoelectric nanobeams and reported that the size effects have significant role in attenuating the vibrations of nanobeams made of piezoelectric materials. Arani and his team have reported compressively on the size effects on the nanobeams made of piezoelectric materials in series of articles pertaining to double walled boron nitride nanotubes (DWBNNTs) conveying fluids, nonlinear analysis of magneto strictive sandwich nanobeams of functionally graded materials, fluid structure interaction of moving sandwich plates with nanoplate facings [40-42]. Mohammadi et al., [43] analyzed the rotating layered nanobeam using the Timoshenko beam model. Arani et al., [44] studied the biaxial in plane forces effect on the frequency analysis of sandwich plates composed of intelligent material layers. Mohammadi et al., [45, 46] studied the Coriolis effect on the rotating multilayer piezoelectric nanobeams during their study on the thermo-mechanical vibration analysis and hygro-thermal vibration analysis of nanobeams on visco-pasternak foundation elastic media. Wan et al., [47] studied the agglomeration effect of CNTs and its waviness on the free, forced vibration, energy absorption and post-buckling analysis of hybrid nanocomposite plates. Al-Furzan at al., [48] studied the wave propagation analysis of micro air wings composed of magnetostrictive layers. Shan et al., [49] carried out the extensive review on the effect of nano-additives on the mechanical impact, post buckling and, the vibration analysis of composite structures. Chu and his team studied the flexoelectric response of nanoplates carrying magnetostrictive layers on frictional torsion medium [50]. Later Chu and his co-authors have studied the energy harvesting behavior of shape memory alloys (SMA) conical panel of nano size embedded with nanoplate piezoelectric layer under moving load and found that the energy harvesting capacity of the nano conical panels are greatly enhanced by the use of piezoelectric layers [51]. Wan et al., [52] studied the flutter effect of supersonic hybrid composite with smart material subjected to yawing. The works reported above shows the versatile use of piezoelectric materials in one form or the other used either for energy storage, or the attenuation the vibration, or the damping of the vibrations of structures. Hence, the need arises of making different types of piezoelectric materials layers and one such step towards the development of the piezoelectric material layer is by Dhala and Ray [53] who were motivated by the works of Lanzara and Chang [20, 22] to estimate the effective piezoelectric and mechanical properties of novel piezoelectric fuzzy fiber reinforced composite (PFFRC). Most of the works in the literature show that the piezoelectric materials layers are used in one form or the other in an application-oriented manner for either attenuation or energy storage purposes. Also, the use of CNTs as reinforcements for enhancing the effective elastic properties of the composites has been the focus of researchers over the past few decades with little work reported on enhancing the effective elastic and also the piezoelectric properties of piezoelectric composites. The review of literature suggests that only a few works have been reported on harnessing the potentiality of the CNTs grown on piezo fibers to estimate the enhanced properties of PFFRCs and hence it provides and ample scope for carrying out further research. The novelty of the present work lies in harnessing the potentiality of the CNTs in enhancing the effective elastic and piezoelectric properties of the piezoelectric composites. Firstly, the earlier works have reported on the use of straight CNTs grown on the base 1-3 piezoelectric fiber and such a fiber is embedded in the matrix to for 1-3 piezoelectric fuzzy fiber reinforced composite (PFFRC). However, the works does not account for the waviness of CNTs which cannot be ignored and no work to the best of authors knowledge has been reported considering the waviness of CNTs on the effective elastic and piezoelectric properties of composites and this is the novel feature and the crux of present study. Also, the earlier study is focused on vertically reinforced 1-3 PFFRC and no study is reported on the horizontally reinforced short piezoelectric fuzzy fiber reinforced composite which also is the novel feature of the present study.

2. Novelty of the present work

Based on the literature review, the novelty of the present work is explained in the following points.

- The study pertaining to use of horizontally reinforced short piezoelectric (PZT) fibers with radially grown CNTs on the periphery of these PZTs considering waviness is not yet reported and hence, the present study

focused towards estimation of elastic and piezoelectric properties of horizontally oriented short piezo fuzzy fiber reinforced composites (SPFFRCs).

- Also, the studies on CNT waviness and its effect on effective elastic and piezoelectric properties of horizontally reinforced SPFFRCs have not been reported yet and is dealt comprehensively in the present study.
- To ensure the no contact between the adjacent CNTs, the CNTs are first modelled as fiber embedded in the interface and the combined CNT and interface is then embedded in the matrix to for the polymer matrix nanocomposite (PMNC). Hence, using the four step three phase micromechanical modelling to estimate the elastic and electrical properties of the horizontally aligned SPFFRCs has not been studied and is the novelty of the present work.

Hence, the present work is aimed at predicting the mechanical and piezo electric properties of horizontally aligned short piezo fuzzy fiber reinforced composites (SPFFRC) using a three-phase micromechanics-based method of cells (MOC) approach.

3. Nomenclature

CNT	Carbon Nanotube
PMNC	Polymer matrix nanocomposite
PZT	Piezoelectric Fiber
PFF	Piezoelectric Fuzzy Fiber
RUC	Repeating Unit Cells
RVE	Representative Volume Element
V	Volume of the Unit cell (RUV)
dnt	Diameter of Carbon Nanotube (nm)
d	Diameter of PZT Fiber (nm)
a	Radius of PZT Fiber (nm)
R	Radius of PFF (nm)
D_b	Diameter of PFF (nm)
M, N	Number of subcells present in the unit cell along the x and y direction, respectively
b, c	Width of the subcell
h, k	Height of the subcell
l_{nt}	Length of carbon nanotube (nm)
L_n	Length between the ends of the nanotube (nm)
L_{pzf}	Length of PZT Fiber (nm)
A_m	Amplitude of CNT wave (nm)
e	Piezoelectric Coefficient (C/m^2)
E_3	Electric field applied across the lamina of composite
p	Number of waves of the wavy carbon nanotube along its longitudinal direction
υ^p, υ^i	Poisson's ratio of PZT fiber and Interface, respectively
ϕ	Angle of waviness
θ	Angle of orientation of CNTs
Superscripts:	
β, γ	Denoting properties of $\beta\gamma^{th}$ subcells.
nc	Nanocomposite
pff	Piezoelectric Fuzzy Fiber
pzt	Piezoelectric Fiber
m	Polymer Matrix
pmnc	Polymer Matrix Nanocomposite
T	Transpose of matrix

Subscripts:	
i	Interphase
nt	Nanotube
f	Fiber

4. Methodology

Figure 1 shows the plan and elevation of the horizontally aligned short piezo fuzzy fiber reinforced composite (SPFFRC) with radially grown wavy CNTs. The short piezo fuzzy fiber (SPFF) are aligned in discontinuous manner longitudinally in direction 1 with CNTs oriented along direction 2. The SPFF is encapsulated within the polymer matrix to form SPFFRC. The CNTs are assumed to be attained a curvature periodic in nature that is modeled as sinusoidal wave. An electric potential is being applied across the thickness of the lamina along the 1-axis i.e. along the longitudinal axis of the piezoelectric fiber which helps to estimate the piezoelectric coefficient of the fiber along with the other elastic properties. The method of cells (MOC) micromechanics approach has been employed in the present study and the repeating unit cell (RUC) pertaining to MOC approach is being depicted in figure 2.

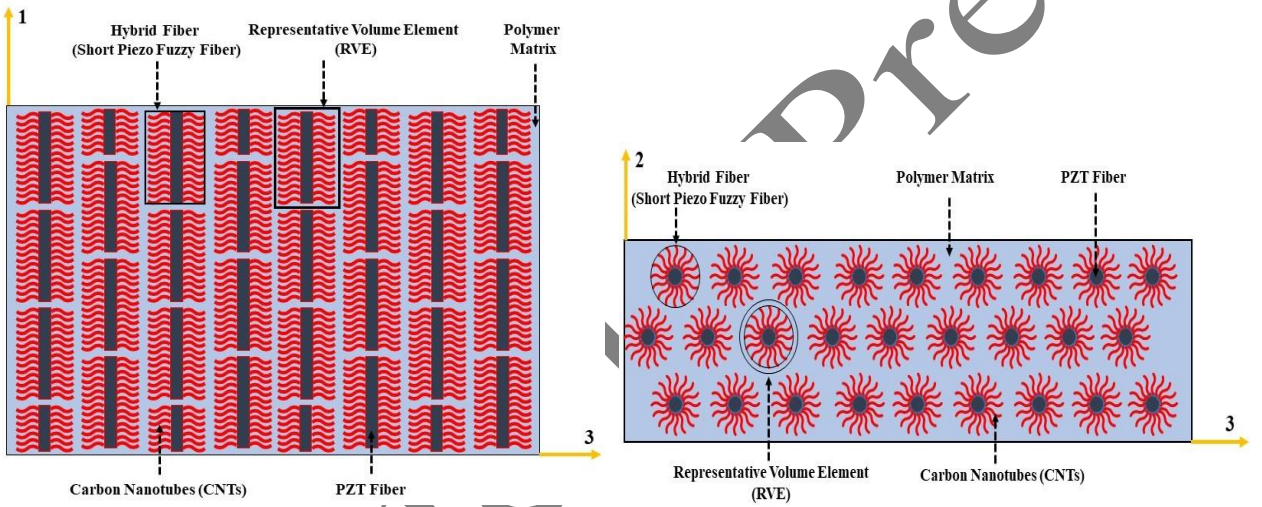

(a) Plan (b) Elevation

Fig 1: Schematic representation of horizontally aligned short piezo fuzzy fiber reinforced composite (SPFFRC) (a) Plan view and (b) Elevation

3.1 *Method of cells approach*:

The method of cells (MOC) approach is a powerful computational technique used for estimating the effective elastic and piezoelectric properties of nanocomposites. The effective elastic properties refer to the overall mechanical behavior of the nanocomposite while piezo electric properties refer to the coupling matrix coefficients between the stress vector and the electric displacement vector. The MOC approach divides the nanocomposite into a finite number of cells called the representative volume element (RVE) or subdomains, each representing a small volume element within the material. The RUC of the typical MOC approach adopted in the present model is displayed in figure 2. As shown in the fig. 2, the phase 1 and the phase 2 constituents of the RUC constitute different materials that combine to form a new entity which will be depicted as phase 1 or phase 2 in the subsequent representation for the next step MOC approach. Similar process is repeated in a four-step manner to obtain the overall properties of the desired SPFFRC and the various steps and the subsequent phases (phase 1 and phase 2) at each step of MOC approach are shown in figure 3. The MOC approach utilizes the concept of homogenization, which estimates the properties of a heterogeneous material on the basis of the properties of its constituent phases.

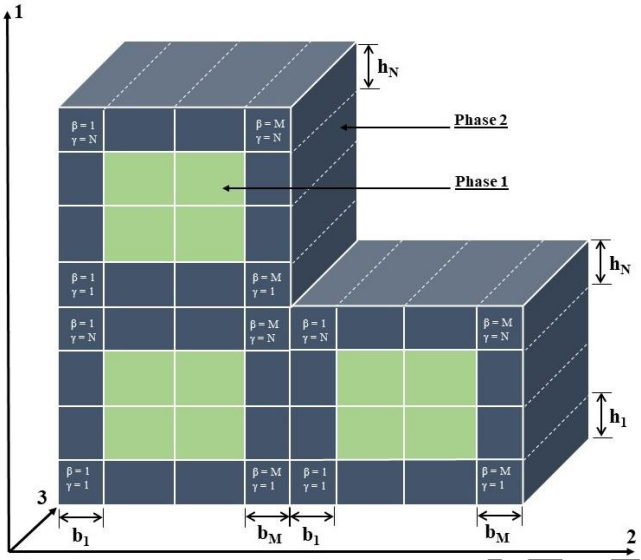

Fig 2: Repeating unit cell (RUC) arrangement in line with the method of cells (MOC) approach.

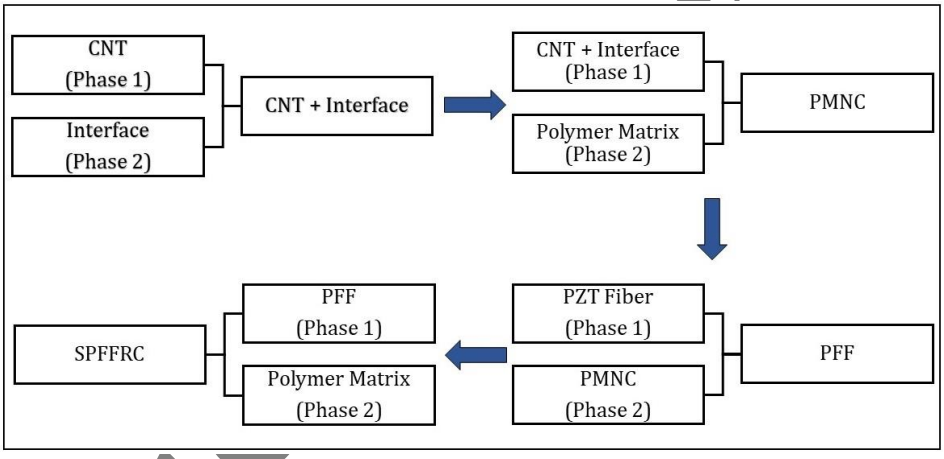

Fig. 3: Schematic representation of various phases corresponding to the RUC constituents for each step MOC approach

Within each cell, the local behavior of the constituents is considered taking both the constituent phases like the matrix and the reinforcements. The interactions between the matrix and the reinforcements are typically represented through appropriate interface conditions. The MOC approach is used to solve the governing equations of elasticity for each cell, considering the continuity requirements at the interfaces between neighboring cells following a set of equations. A three phase MOC approach has been employed to estimate the elastic and piezoelectric properties SPFFRC. In the first step, the CNTs embedded in the interface and then the combined CNT and interphase form the phase 1 of the next step RUC representation while matrix is considered as phase 2 and both are combined to obtain the polymer matrix nanocomposite (PMNC). Next, the base piezo fiber which constitute phase 1 is embedded in the PMNC which constitute to phase 2 of the second step RUC where PMNC is the matrix phase while piezo fiber being the reinforcement phase leading the piezo fuzzy fiber (PFF). The PFF which becomes phase 1 is then embedded in the matrix which is phase 2 in the third stage RUC to form the desired SPFFRC. The PFF is reinforced horizontally in a discontinuous manner in the conventional epoxy to obtain the horizontally aligned short piezo fuzzy fiber reinforced composite (SPFFRC). The following displacement continuity and traction continuity equations are used at the individual steps to obtain the overall properties of the SPFFRCs. The displacement continuity equations ensure that the displacements of neighboring cells within a material interface are continuous and are shown below [54]

$$\left.\begin{aligned}
&\sum_{\beta=1}^{M} b_\beta \varepsilon_1^{\beta\gamma} = b\varepsilon_1^{nc} \quad \gamma = 1,2,.....,N, \quad \sum_{\gamma=1}^{N} h_\gamma \varepsilon_2^{\beta\gamma} = h\varepsilon_2^{nc} \quad \beta = 1,2,....,M \\
&\varepsilon_3^{\beta\gamma} = \varepsilon_3 \quad \beta = 1,2,....,M, \quad \gamma = 1,2,.....,N \\
&\sum_{\gamma=1}^{N} h_\gamma \varepsilon_{23}^{\beta\gamma} = h\varepsilon_{23}^{nc} \quad \beta = 1,2,....,M, \quad \sum_{\beta=1}^{M} b_\beta \varepsilon_{13}^{\beta\gamma} = b\varepsilon_{13}^{nc} \quad \gamma = 1,2,.....,N, \\
&\sum_{\beta=1}^{M}\sum_{\gamma=1}^{N} b_\beta h_\gamma \varepsilon_{12}^{\beta\gamma} = bh\varepsilon_{12}^{nc}
\end{aligned}\right\} \tag{1}$$

Similar to the above discontinuity equations, (5MN - 2M - 2N -1) number of equations ensures relationship between the stresses in sub cells considering the continuity in traction condition [54]

$$\left.\begin{aligned}
&\sigma_1^{\beta\gamma} = \sigma_1^{(\beta+1)\gamma} \quad \text{where } \beta = 1,2,.....(M-1) \text{ and } \gamma = 1,2,.....N \\
&\sigma_2^{\beta\gamma} = \sigma_2^{\beta(\gamma+1)} \quad \text{where } \beta = 1,2,.....M \text{ and } \gamma = 1,2,.....(N-1) \\
&\sigma_{13}^{\beta\gamma} = \sigma_{13}^{(\beta+1)\gamma} \quad \text{where } \beta = 1,2,.....(M-1) \text{ and } \gamma = 1,2,.....N \\
&\sigma_{23}^{\beta\gamma} = \sigma_{23}^{\beta(\gamma+1)} \quad \text{where } \beta = 1,2,.....M \text{ and } \gamma = 1,2,.....(N-1) \\
&\sigma_{12}^{\beta\gamma} = \sigma_{12}^{(\beta+1)\gamma} \quad \text{where } \beta = 1,2,.....(M-1) \text{ and } \gamma = 1,2,.....N \\
&\sigma_{12}^{\beta\gamma} = \sigma_{12}^{\beta(\gamma+1)} \quad \text{where } \beta = 1 \text{ and } \gamma = 1,2,.....N-1
\end{aligned}\right\} \tag{2}$$

Arranging the above set of displacement continuity equations, and the set of traction continuity equations in the matrix form results in the following equation shown below

$$[A]\{\varepsilon\}^{\beta\gamma} = [B]\{\varepsilon\}^{nc} \tag{3}$$

This global matrix contains elastic properties as well as the geometrical properties of the respective phases namely, CNTs, polymer matrix, and interphase that form the final PMNC after step 1. The same equation is rearranged to get strain vector for the constituent phases as follows

$$\{\varepsilon\}^{\beta\gamma} = \left[A_c\right]^{\beta\gamma} \{\varepsilon\}^{nc} \text{ with } [A_c]^{\beta\gamma} = \frac{[B]}{[A]} \tag{4}$$

Since the stress and strain vectors have been obtained, the constitutive equations of the polymer matrix nanocomposite (PMNC) can be obtained as

$$\left\{\sigma^{nc}\right\} = \left[C^{nc}\right]\left\{\varepsilon^{nc}\right\} \tag{5}$$

By comparing all the above equations, matrix with the elements as the effective elastic coefficients for the PMNC are generated and are as follows

$$\left[\mathrm{C^{nc}}\right] = \frac{1}{\mathrm{V}}\sum_{\beta=1}^{\mathrm{M}}\sum_{\gamma=1}^{\mathrm{N}} \mathrm{V}_{\beta\gamma}\left[\mathrm{C^{\beta\gamma}}\right]\left[\mathrm{A_c^{\beta\gamma}}\right] \tag{6}$$

Equation (6) gives the effective elastic coefficient matrix consist of the effective elastic properties located at a point in the PMNC which is embedded around the piezoelectric fiber. According to the local coordinate system of matrix which is surrounding the fiber as well as the reinforcing nanotube which is aligned with the 3-axis. At a position in the PMNC where the CNT axis is oriented at an angle ‘θ’ with the 3-axis, the matrix also offers the elastic characteristics in the same direction. The representative volume element (RVE) of the three phase cross sections of the SPFFRC is schematically represented in figure 4. Figure 4(a) depicts the section view of the CNT grown horizontally reinforced short piezo fiber with waviness oriented in 2-3 plane while figure 3(b) shows the orientation of the CNTs in the 1-3 plane.

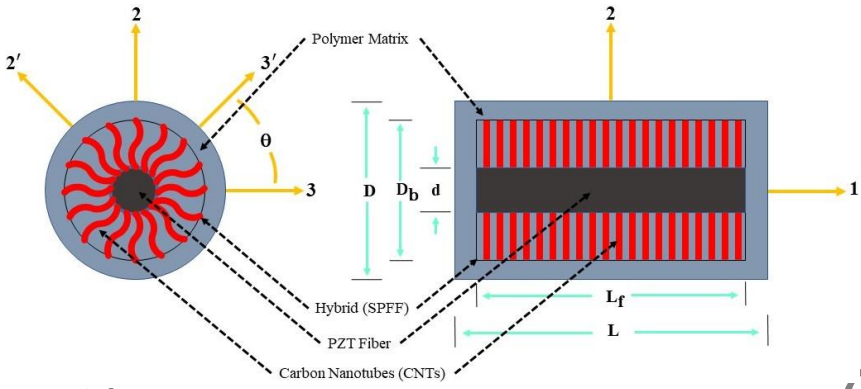

(a) Waviness of CNTs along the 2-3 plane.

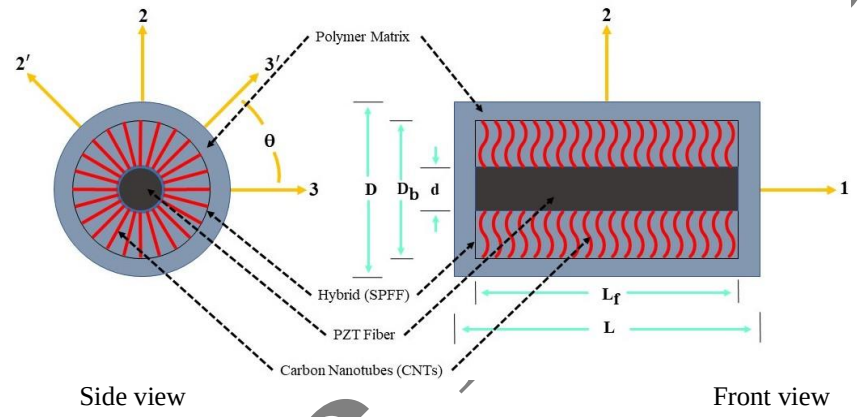

(b) Waviness of CNTs along the 1-3 plane.

Fig. 4: Cross-sections of the three-phase RVE of the Short piezo fuzzy fiber with radially grown wavy CNTs (a) waviness of CNTs along 2-3 plane and (b) waviness of CNTs along 1-3 plane.

The effective elastic constants following the amplitude of the sinusoidal curve created by CNT is coplanar with the 1-3 plane are given as follows

$$
\begin{aligned}
&C_{11}^{NC} = C_{11}^{nc} f^4 + C_{33}^{nc} g^4 + 2\left(C_{13}^{nc} + 2C_{55}^{nc}\right) f^2 g^2;\ C_{12}^{NC} = C_{12}^{nc} f^2 + C_{23}^{nc} g^2 \\
&C_{13}^{NC} = \left(C_{11}^{nc} + C_{33}^{nc} - 4C_{55}^{nc}\right) f^2 g^2 + C_{13}^{nc}\left(f^4 + g^4\right);\ C_{22}^{NC} = C_{22}^{nc};\ C_{23}^{NC} = C_{12}^{nc} g^2 + C_{23}^{nc} f^2 \\
&C_{33}^{NC} = C_{11}^{nc} g^4 + C_{33}^{nc} f^4 + 2\left(C_{13}^{nc} + 2C_{55}^{nc}\right) f^2 g^2;\ C_{44}^{NC} = C_{44}^{nc} f^2 + C_{66}^{nc} g^2 \\
&C_{55}^{NC} = \left(C_{11}^{nc} + C_{33}^{nc} - 2C_{13}^{nc} - 2C_{55}^{nc}\right) f^2 g^2 + C_{55}^{nc}\left(f^4 + g^4\right);\ C_{66}^{NC} = C_{44}^{nc} g^2 + C_{66}^{nc} f^2
\end{aligned}
\tag{7}
$$

While the same for CNTs coplanar with the 2-3 plane are given by

$$
\begin{aligned}
&C_{11}^{NC} = C_{11}^{nc};\ C_{22}^{NC} = C_{22}^{nc} f^4 + C_{33}^{nc} g^4 + 2\left(C_{23}^{nc} + 2C_{44}^{nc}\right) f^2 g^2 \\
&C_{12}^{NC} = C_{12}^{nc} f^2 + C_{13}^{nc} g^2;\ C_{23}^{NC} = \left(C_{22}^{nc} + C_{33}^{nc} - 4C_{44}^{nc}\right) f^2 g^2 + C_{23}^{nc}\left(f^4 + g^4\right) \\
&C_{33}^{NC} = C_{22}^{nc} g^4 + C_{33}^{nc} f^4 + 2\left(C_{23}^{nc} + 2C_{44}^{nc}\right) f^2 g^2 \\
&C_{44}^{NC} = \left(C_{22}^{nc} + C_{33}^{nc} - 2C_{23}^{nc} - 2C_{44}^{nc}\right) f^2 g^2 + C_{44}^{nc}\left(f^4 + g^4\right);\ C_{55}^{NC} = C_{55}^{nc} f^2 + C_{66}^{nc} g^2 \\
&C_{66}^{NC} = C_{55}^{nc} g^2 + C_{66}^{nc} f^2;\ C_{13}^{NC} = C_{12}^{nc} g^2 + C_{13}^{nc} f^2
\end{aligned}
\tag{8}
$$

$$f = \cos(\phi) = \left(\sqrt{1 + \left\{ \frac{p\pi A_m}{l_{nt}} \times \cos\left(\frac{p\pi y}{l_{nt}} \right) \right\}^2} \right)^{\frac{-1}{2}} \text{ and}$$

Where, (9)

$$g = \sin(\phi) = \frac{p\pi A_m}{l_{nt}} \times \cos\left(\frac{p\pi y}{l_{nt}} \right) \left(\sqrt{1 + \left\{ \frac{p\pi A_m}{l_{nt}} \times \cos\left(\frac{p\pi y}{l_{nt}} \right) \right\}^2} \right)^{\frac{-1}{2}}$$

Where, A_m is the amplitude of the CNT wave, 'p' is the number of waves and l_{nt} is the length of the carbon nanotube. The effective coefficients for the length of the CNT are derived by averaging the matrix produced by the equations over the linear distance (L_n) between the ends of the CNT.

$$\left[\overline{C}_{wavy} \right] = \frac{1}{L_n} \int_0^{l_{nt}} \left[C^{NC} \right] dy \tag{10}$$

$[\overline{C}_{wavy}]$ matrix gives point-specific elastic property values. However, the matrix $[\overline{C}_{wavy}]$ also offers the properties at different orientations with respect to the local coordinate system, therefore the point-dependent elastic properties were determined using the transformation matrix [T]. Similarly, the orientation of carbon nanotubes is thought to diverge from their longitudinal axis as waviness in CNT is introduced, the effective elastic coefficients so obtained using Eq. (10) are further deduced by applying the relevant transformations mentioned below.

$$\left[\overline{C}_{nc} \right] = [T]^{-1} \left[\overline{C}_{wavy} \right] [T]^{-T} \text{ with } [\mathrm{T}] = \begin{bmatrix} \mathrm{m}^2 & \mathrm{n}^2 & 0 & 0 & 0 & -\mathrm{mn} \\ \mathrm{n}^2 & \mathrm{m}^2 & 0 & 0 & 0 & \mathrm{mn} \\ 0 & 0 & 1 & 0 & 0 & 0 \\ 0 & 0 & 0 & \mathrm{m} & \mathrm{n} & 0 \\ 0 & 0 & 0 & -\mathrm{n} & \mathrm{m} & 0 \\ 2\mathrm{mn} & -2\mathrm{mn} & 0 & 0 & 0 & \mathrm{m}^2 - \mathrm{n}^2 \end{bmatrix} \tag{11}$$

Here, $\mathrm{m} = \cos(\theta)$ and $\mathrm{n} = \sin(\theta)$, respectively. Equation (11) consequently yields values for the effective elastic property that are particular to a point in the lamina of PMNC. Additionally, because the properties do change with circumferential enhancement, the effective property must be integrated into the circumferential boundaries in order to produce location-dependent effective elastic characteristics, as indicated below

$$C_{pmnc} = \frac{1}{\pi \left(R^2 - a^2 \right)} \int_0^{2\pi} \int_a^R \left[\overline{C}_{pmnc} \right] r dr d\theta \tag{12}$$

When executing further formulations in the context of piezo fuzzy fibre (PFF), a similar pattern described earlier has been followed. Since the nanotubes are radially embedded to the circumferential surface of the fibres, creating a PFF, in accordance with the unique structure, they are perpendicularly orientated. Since these components are joined together by a polymer matrix, they form a nanocomposite made of fibre and polymer matrix. In order to determine the PFFs effective properties, the PMNC properties are predicted after which the fibre's properties are used. The formulation for the PFF part is as follows [53]

$$\left\{ e^{\beta\gamma} \right\} = \left[e_{31}^{\beta\gamma} \quad e_{32}^{\beta\gamma} \quad e_{33}^{\beta\gamma} \quad 0 \quad 0 \quad 0 \right]^T \tag{13}$$

The RUC's subcell locations are indicated by the superscript 'βγ' which denotes the phases of the relevant constituent in which PZT refers to piezoelectric fibre and PMNC refers for polymer matrix nanocomposite. The PFF's volume averaged stresses and strains are stated as

$$\left\{ \varepsilon^{pff} \right\} = \frac{1}{V} \sum_{\beta=1}^{M} \sum_{\gamma=1}^{N} V_{\beta\gamma} \left\{ \varepsilon^{\beta\gamma} \right\} \text{ and } \left\{ \sigma^{pff} \right\} = \frac{1}{V} \sum_{\beta=1}^{M} \sum_{\gamma=1}^{N} V_{\beta\gamma} \left\{ \sigma^{\beta\gamma} \right\} \tag{14}$$

Following the procedure described earlier in deriving the effective coefficient so PMNC, the same procedure is adopted in step 2, the equations for displacement continuity from between the neighboring cells of PZT and PMNC at a material interface and the traction continuity was depicted for PFF when PMNC was taken into consideration, the (5MN - 2M - 2N - 1) number of equations ensures a link between the stresses in sub cells are given as follows [54]

$$\left.\begin{array}{l} \varepsilon_1^{\beta\gamma} = \varepsilon_1^{pff} \quad \beta = 1,2,.....M, \quad \gamma = 1,2,.....N, \quad \sum_{\gamma=1}^{N} k_\gamma \varepsilon_2^{\beta\gamma} = k\varepsilon_2^{pff} \quad \beta = 1,2,.....M \\ \sum_{\beta=1}^{M} c_\beta \varepsilon_3^{\beta\gamma} = c\varepsilon_3^{pff} \quad \gamma = 1,2,.....N, \quad \sum_{\beta=1}^{M}\sum_{\gamma=1}^{N} c_\beta k_\gamma \varepsilon_{23}^{\beta\gamma} = ck\varepsilon_{23}^{pff} \\ \sum_{\gamma=1}^{N} k_\gamma \varepsilon_{12}^{\beta\gamma} = k\varepsilon_{12}^{pff} \quad \beta = 1,2,.....M, \quad \sum_{\beta=1}^{M} c_\beta \varepsilon_{13}^{\beta\gamma} = c\varepsilon_{13}^{pff} \quad \gamma = 1,2,.....N \end{array}\right\} \text{ and}$$

$$\left.\begin{array}{lll} \sigma_3^{\beta\gamma} = \sigma_3^{(\beta+1)\gamma} & \beta = 1,2,.....M-1, & \gamma = 1,2,.....N \\ \sigma_2^{\beta\gamma} = \sigma_2^{\beta(\gamma+1)} & \beta = 1,2,.....M, & \gamma = 1,2,.....N-1 \\ \sigma_{23}^{\beta\gamma} = \sigma_{23}^{(\beta+1)\gamma} & \beta = 1,2,.....M-1, & \gamma = 1,2,.....N \\ \sigma_{23}^{\beta\gamma} = \sigma_{23}^{\beta(\gamma+1)} & \beta = 1, & \gamma = 1,2,.....N-1 \\ \sigma_{13}^{\beta\gamma} = \sigma_{13}^{(\beta+1)\gamma} & \beta = 1,2,.....M-1, & \gamma = 1,2,.....N \\ \sigma_{12}^{\beta\gamma} = \sigma_{12}^{\beta(\gamma+1)} & \beta = 1,2,.....M, & \gamma = 1,2,.....N-1 \end{array}\right\} \quad (15)$$

The afore mentioned set of equations are arranged in the matrix form to obtain the following

$$[A_D]\{\varepsilon_s\} = [B]\{\varepsilon^{pff}\} \quad (16)$$

In which $[A_D]$ is the [(2(M + N) + MN + 1) X (6MN)] matrix composed of the geometrical parameters of the subcells, and [B] is the matrix formed by the geometrical parameters of the cell. $\{\varepsilon_s\}$ is the (6MN X 1) vector of sub cell strains compiled together, and $\{\varepsilon^{pff}\}$ is the (6X1) vector of the PFF fiber strain while the traction continuity criteria are arranged in a matrix form as

$$[A_T]\{\varepsilon_s\} - \{e_s\}E_3 = 0 \quad (17)$$

In which $[A_T]$ is a [(5MN - 2(M+N) -1) X (6MN)] matrix containing the elastic properties of the subcells, and $\{e_s\}$ is the [(5MN - 2(M+N) - 1) X 1] piezoelectric coefficient vector of the subcells joined together. A global matrix is obtained by combining the two aforementioned Eqs. (16) and (17) and is as follows.

$$[A]\{\varepsilon_s\} = [K]\{\varepsilon^{pff}\} + [D]E_3; \text{ where } [A] = \begin{bmatrix}[A_D]\\ [A_T]\end{bmatrix}, [K] = \begin{bmatrix}[B]\\ [\bar{0}]\end{bmatrix}, \{D\} = \begin{bmatrix}\{\hat{0}\}\\ \{e_s\}\end{bmatrix} \quad (18)$$

With $[\bar{0}]$ and $\{\hat{0}\}$ being [(5MN - 2(M + N) - 1) X 6] and [(2(M + N) + MN + 1) X 1] null vectors, respectively. The subcell strains can be expressed as the composite strain as follows.

$$\{\varepsilon_s\} = [A_M]\{\varepsilon^{pff}\} + \{D_M\}E_3; \text{ where } [A_M] = [A]^{-1}[K] \text{ and } \{D_M\} = [A]^{-1}\{D\} \quad (19)$$

The strain concentration factors for each subcell may now be acquired from the matrices $[A_M]$ and $\{D_M\}$, respectively, allowing for the expression of each subcell strain as.

$$\{\varepsilon^{\beta\gamma}\} = [A_M^{\beta\gamma}]\{\varepsilon^{pff}\} + \{D_M^{\beta\gamma}\}E_3 \quad (20)$$

Substituting eq (20) into constitutive equation, yields

$$\{\sigma^{\beta\gamma}\} = [C^{\beta\gamma}]\left([A_M^{\beta\gamma}]\{\varepsilon^{pff}\} + \{D_M^{\beta\gamma}\}E_3\right) - \{e^{\beta\gamma}\}E_3 \quad (21)$$

The constitutive relation for the piezo fuzzy fiber (PFF) can be constructed as follows.

$$\{\sigma^{pff}\} = [C^{pff}]\{\varepsilon^{pff}\} - \{e^{pff}\}E_3 \quad (22)$$

where the PFF effective elastic coefficient matrix $[C^{pff}]$ and effective piezoelectric coefficient vector $\{e^{pff}\}$ are given by

$$[C^{pff}] = \frac{1}{V}\sum_{\beta=1}^{M}\sum_{\gamma=1}^{N} V_{\beta\gamma}[C^{\beta\gamma}][A_M^{\beta\gamma}] \text{ and } \{e^{pff}\} = \frac{1}{V}\sum_{\beta=1}^{M}\sum_{\gamma=1}^{N} V_{\beta\gamma}\left([C^{\beta\gamma}]\{D_M^{\beta\gamma}\} - \{e^{\beta\gamma}\}\right) \quad (23)$$

The generalized method of cell approach previously described for the PFF is then appropriately enhanced to derive the constitutive relation of the horizontally reinforced SPFFRC. This is done by using the elements of the

PFF as the parameters of the reinforcement along the 3-direction and the polymer as the matrix material with the stress strain constitutive equations given by

$$\{\sigma\} = [C]\{\varepsilon\} - \{e\}E_3 \tag{24}$$

In the equation above, [C] and {e} are the effective elastic coefficient matrix and the effective piezoelectric coefficient vector of the SPFFRC, respectively. Likewise, {σ} and {ε} are the states of stress and strain in the homogenized SPFFRC.

2.2 Mori and Tanaka method [55]:

The results obtained from the MOC approach are then compared with the existing and widely used analytical model called the Mori Tanaka (MT) method. This method assumes that the composite material consists of a homogeneous matrix phase containing dispersed inclusions and the constitutive material matrix is given by [29, 55, 56]

$$\left[C^{nc}\right] = \left[C^{m}\right] + \frac{\left[\left(v_{nt}+v_i\right)\left(\left[C^{i}\right]-\left[C^{m}\right]\right)[A_v] + v_{nt}\left(\left[C^{nt}\right]-\left[C^{i}\right]\right)[A_{nt}]\right]}{v_m[I] + \left(v_{nt}+v_i\right)[A_v]} \tag{25}$$

where $[\mathrm{A_v}] = [\mathrm{I}] + [\mathrm{S_v}][\phi_v]$, $[\mathrm{A_{nt}}] = [\mathrm{I}] + [\Delta\mathrm{S}][\phi_i] + [\mathrm{S_{nt}}][\phi_{nt}]$

with $[\phi_{nt}] = -\left[\left(\left[\mathrm{S_{nt}}\right]+\left[\mathrm{C^1}\right]\right) + [\Delta\mathrm{S}]\left(\left[\mathrm{S_{nt}}\right] - \frac{\mathrm{v_{nt}}}{\mathrm{v_i}}[\Delta\mathrm{S}] + \left[\mathrm{C^1}\right]\right)\left(\left[\mathrm{S_{nt}}\right] - \frac{\mathrm{v_{nt}}}{\mathrm{v_i}}[\Delta\mathrm{S}] + \left[\mathrm{C^2}\right]\right)^{-1}\right]^{-1}$

and $[\phi_i] = -\left[(\Delta\mathrm{S}) + \left(\left[\mathrm{S_{nt}}\right]+\left[\mathrm{C^1}\right]\right)\left(\left[\mathrm{S_{nt}}\right] - \frac{\mathrm{v_{nt}}}{\mathrm{v_i}}[\Delta\mathrm{S}] + \left[\mathrm{C^2}\right]\right)\left(\left[\mathrm{S_{nt}}\right] - \frac{\mathrm{v_{nt}}}{\mathrm{v_i}}[\Delta\mathrm{S}] + \left[\mathrm{C^1}\right]\right)^{-1}\right]^{-1}$

$$[\Delta S] = [S_{nt}] - [S_v];\ \left[C^1\right] = \left(\left[C^{nt}\right] - \left[C^{m}\right]\right)^{-1}\left[C^{m}\right];\ \left[C^2\right] = \left(\left[C^{i}\right] - \left[C^{m}\right]\right)^{-1}\left[C^{m}\right] \tag{26}$$

The Eshelby tensors for the domains 'n' and 'V' are denoted in the aforementioned matrices by $[\mathrm{S_{nt}}]$ and $[\mathrm{S_v}]$, respectively. The CNT may be regarded as a solid circular cylinder, as inferred in the MT model. As a result, the matrices $[\mathrm{S_{nt}}]$ and $[\mathrm{S_v}]$ are computed using the special version of the Eshelby tensor for cylindrical inclusion as given by Qui and Weng [56]. The following specifically composed formulas as shown in equation (27), represent the constituents of the Eshelby tensor for the cylindrical CNT reinforcement in the isotropic interphase and the cylindrical volume (V) made up of the CNT and the interphase in the isotropic polymer matrix. The elements of Eshelby tensor in which ν^p and ν^i stand for the PZT fiber's and the interphase's respective Poisson's ratios are defined as.

$$[S_n] = \begin{bmatrix} S^n_{1111} & S^n_{1122} & S^n_{1133} & 0 & 0 & 0 \\ S^n_{2211} & S^n_{2222} & S^n_{2233} & 0 & 0 & 0 \\ S^n_{3311} & S^n_{3322} & S^n_{3333} & 0 & 0 & 0 \\ 0 & 0 & 0 & S^n_{2323} & 0 & 0 \\ 0 & 0 & 0 & 0 & S^n_{1313} & 0 \\ 0 & 0 & 0 & 0 & 0 & S^n_{1212} \end{bmatrix} \text{ and } [S_v] = \begin{bmatrix} S^v_{1111} & S^v_{1122} & S^v_{1133} & 0 & 0 & 0 \\ S^v_{2211} & S^v_{2222} & S^v_{2233} & 0 & 0 & 0 \\ S^v_{3311} & S^v_{3322} & S^v_{3333} & 0 & 0 & 0 \\ 0 & 0 & 0 & S^v_{2323} & 0 & 0 \\ 0 & 0 & 0 & 0 & S^v_{1313} & 0 \\ 0 & 0 & 0 & 0 & 0 & S^v_{1212} \end{bmatrix} \tag{27}$$

$$\left.\begin{aligned}
&S^n_{1111}=S^n_{2222}=\left\{\left(5-4\nu^i\right)\Big/8\left(1-\nu^i\right)\right\},\ S^n_{1122}=S^n_{2211}=\left\{\left(4\nu^i-1\right)\Big/8\left(1-\nu^i\right)\right\}\\
&S^n_{1212}=\left\{\left(3-4\nu^i\right)\Big/8\left(1-\nu^i\right)\right\},\ S^n_{1133}=S^n_{2233}=\left\{\nu^i\Big/2\left(1-\nu^i\right)\right\}\\
&S^n_{1313}=S^n_{2323}=\left\{1\Big/4\right\},\ S^v_{1111}=S^v_{2222}=\left\{\left(5-4\nu^p\right)\Big/8\left(1-\nu^p\right)\right\},\ S^v_{1133}=S^v_{2233}=\left\{\nu^p\Big/2\left(1-\nu^p\right)\right\}\\
&S^v_{1122}=S^v_{2211}=\left\{\left(4\nu^p-1\right)\Big/8\left(1-\nu^p\right)\right\},\ S^v_{1212}=\left\{\left(3-4\nu^p\right)\Big/8\left(1-\nu^p\right)\right\}\\
&S^v_{1313}=S^v_{2323}=\left\{1\Big/4\right\},\ S^n_{3333}=S^n_{3311}=S^n_{3322}=S^v_{3333}=S^v_{3311}=S^v_{3322}=0
\end{aligned}\right\} \tag{28}$$

The PFF properties are then estimated using the MT approach in a similar fashion once the effective PMNC properties have been determined.

$$\left[C^{pff}\right]=\left[C^{pmnc}\right]+v_p\left(\left[C^p\right]-\left[C^{pmnc}\right]\right)[A_2] \text{ with } [A_2]=\left[A_2\right]\left[v_{pmnc}[I]+v_p\left[A_2\right]\right]^{-1}$$
$$\text{and}\left[A_2\right]=\left[[I]+[S_2]\left[C^{pmnc}\right]^{-1}\left(\left[C^p\right]-\left[C^{pmnc}\right]\right)\right]^{-1} \tag{29}$$

The strain concentration variables described above could be used to calculate the piezoelectric coefficient vector as shown below.

$$\left\{e^{pff}\right\}=v_p\left[A_2\right]^T\left\{e^p\right\} \tag{30}$$

Then, using the MT approach with the cylindrical PFF implanted in the polymer matrix as reinforcement, the effective elastic and piezoelectric properties of the SPFFRC were able to be again evaluated.

$$[C]=\left[C^m\right]+v_{pff}\left(\left[C^{pff}\right]-\left[C^m\right]\right)[A_3] \text{ with } \left[A_3\right]=\left[A_3\right]\left[v_m[I]+v_{pff}\left[A_3\right]\right]^{-1}$$
$$\textit{and}\left[A_3\right]=\left[[I]+[S_3]\left[C^m\right]^{-1}\left(\left[C^{pff}\right]-\left[C^m\right]\right)\right]^{-1} \tag{31}$$

Where, V_m and V_{pff}, stand for the corresponding volume fractions of the matrix and PFF.

$$\{e\}=v_{pff}\left[A_3\right]^T\left\{e^{pff}\right\} \tag{32}$$

$$\text{While } [S_2]=\begin{bmatrix}
S^{pff}_{1111} & S^{pff}_{1122} & S^{pff}_{1133} & 0 & 0 & 0\\
S^{pff}_{2211} & S^{pff}_{2222} & S^{pff}_{2233} & 0 & 0 & 0\\
S^{pff}_{3311} & S^{pff}_{3322} & S^{pff}_{3333} & 0 & 0 & 0\\
0 & 0 & 0 & S^{pff}_{2323} & 0 & 0\\
0 & 0 & 0 & 0 & S^{pff}_{1313} & 0\\
0 & 0 & 0 & 0 & 0 & S^{pff}_{1212}
\end{bmatrix} \tag{33}$$

5. Results and discussions:

The short piezo fuzzy fiber reinforced composite (SPFFRC) is a novel smart material whose elastic and piezoelectric property have been estimated in the present work. The piezoelectric fiber with radially grown CNTs called as piezo fuzzy fiber is used and reinforcement in the conventional matrix to obtain the elastic and piezoelectric properties. The constituents of the SPFFRC include piezoelectric fiber, polymer matrix, and the carbon nanotubes (CNTs). The material properties of various constituent phases that constitute the SPFFRC are shown in Table 1 [53]. In this study, the composite's general properties are estimated using the value of CNT (5,0). The diameter of the piezoelectric fiber is expected to be 10 μm. The volume percentage of CNTs also predominates as a crucial metric for property estimation since it plays a significant impact in the properties. The root to root surface distance between two neighboring nanotubes, the nanotube diameter, and the fiber diameter all play major roles in determining the carbon nanotube volume fraction (V_{cnt}).

Table 1: Material properties of the constituent phases of SPFFRC in (GPa) [53]

Material	C_{11} (GPa)	C_{12} (GPa)	C_{23} (GPa)	C_{33} (GPa)	C_{55} (GPa)	e_{31} (C/m^2)	e_{33} (C/m^2)	(nm)
CNT (5,0) [8]	3562	409.5	193.7	1587	1537	-	-	dnt = 0.39
CNT (10,0) [8]	1857	165.8	377.2	551.4	787.7	-	-	dnt = 0.78
PZT [4]	121	75.4	75.2	111	21.1	-5.4	9.5	d = 10000
Polyimide [4]	8	4.4	4.4	8	1.8	-	-	-

Only when there is no other material between two neighboring nanotubes is the vanderwals distance, which is roughly 0.34 nm, taken into consideration as the minimum root distance. In this instance, the polymer matrix fills the space between two adjacent CNTs. The minimum distance taken into consideration is 1.7 nm. The geometrical RVE specifications for the SPFFRC are taken as d=10μm, L_f/d=10, L/L_f =1.1 and D/D_b =1.1. The best packing for fibers with a maximum fiber volume fraction of 0.9069 has been determined to be a hexagonal array and the same is displayed in fig. 5 [28]. Determining the volume proportion of CNT is important since the density of carbon nanotubes depends on the structural characteristic of the entire composite and the existence of the same affects the composite properties. The diameter of the nanotube and the distance from the root to the root of two neighboring nanotubes are needed to calculate the maximum volume fraction of the nanotubes that have grown over the surface of the fiber is given by the following equation

$$\left(V_{cnt}\right)_{\max} = \left\{ \pi d_{nt}^2 \Big/ 2\left(d_{nt}+1.7\right)^2 \right\} \left(B_b - 1\right) V_{pzf} \tag{34}$$

where, 'd_{nt}' is the diameter of the CNT and V_{pzf} is the volume fraction of the fiber. Eq. (34) has been derived considering the RVE of nanocomposite as triangle and the derivation has been performed for the same which is shown in Appendix. A PFF is a fascinating and innovative nanomaterial that combines the unique properties of the piezoelectric fibers, CNTs, and the polymer matrix. This arrangement involves the integration of these advanced materials to form a novel and multifunctional structure with potential applications in various cutting-edge technologies. The arrangement of the PFF in a hexagonal packing array shown in fig. 5 is strategically chosen to optimize their mechanical and electrical performance. The hexagonal close-packed structure ensures efficient use of space and provides a continuous network of CNTs and piezoelectric fibers throughout the material.

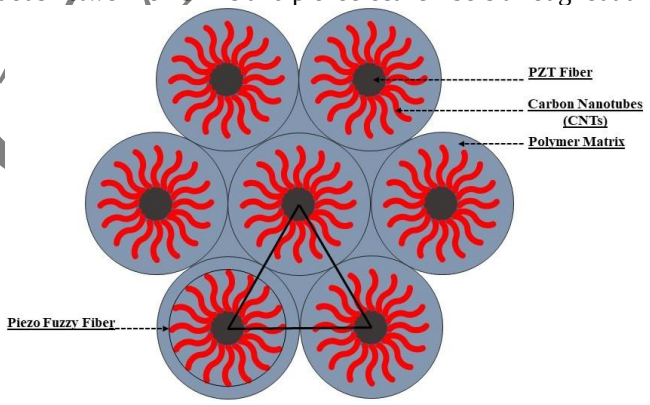

Fig. 5: Piezo fuzzy fiber (PFF) arrangement in a hexagonal packing array

This arrangement maximizes the contact and bonding between neighbouring fibers, leading to improved load distribution and mechanical properties. The aforesaid Eq. (34) enables us to analyse that no nanotube will exist if there is no fibre, and when $V_{pzf} = \pi/2\sqrt{3}$, the volume fraction of the nanotube once more equals zero, enabling the absence of PMNC. As a result, we observed that the greatest volume fraction will fall between values of 0.1 and $\pi/2\sqrt{3}$. The number of fibres will grow as the volume of the fibre increases, which will shorten the length of the

nanotubes. After reaching a maximum volume fraction, this will reduce the CNT volume fraction in the composite. As a result, the value of the maximum volume percentage of CNTs must be computed for a specific value of V_{pzf} in order to determine the overall properties.

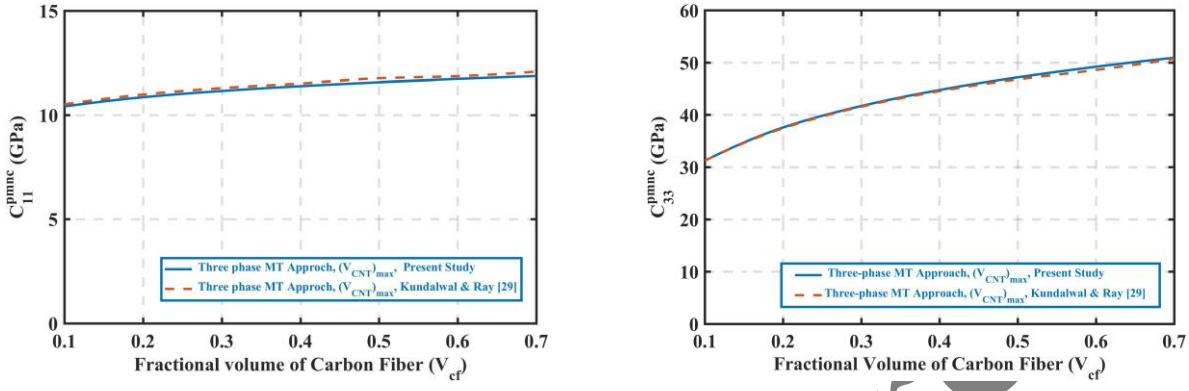

(a) C_{11}^{pmnc} (b) C_{33}^{pmnc}

Fig. 6: Validation of elastic properties of polymer matric nanocomposite (PMNC) (a) C_{11}^{pmnc} and (b) C_{33}^{pmnc} .

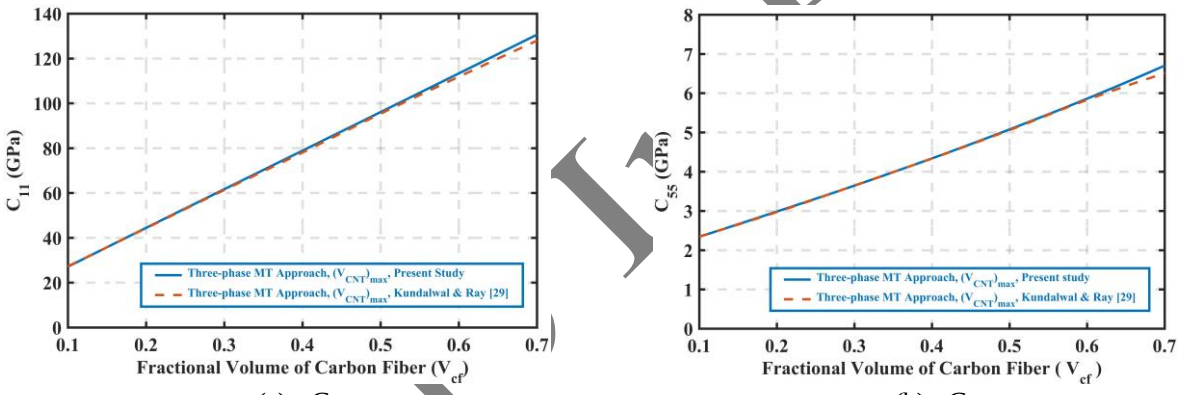

(a) C_{11} (b) C_{55}

Fig. 7: Validation of effective elastic properties of carbon fuzzy fiber reinforced composite (FFRC) (a) C_{11} and (b) C_{55} .

In order establish the current model, the results obtained by the derived micromechanical model are validated first with the similar materials work existing in the open literature [29] and the same are displayed in figures 6 and 7. The results displayed in Figs. 6 and 7 shows the good agreement with those of Kundalwal and Ray [29]. The current work is focussed on orientation variation to examine the effects of waviness of CNTs on the overall properties of the nanocomposite. Nanotube attains the curvature with random orientation for which analytical examination of elastic results are complex and need extreme attention. But for the ease of mathematical calculation, curvatures are assumed to be sine or cosine functions. The variation in orientation of CNT is considered in such a way that the amplitude of the curvature is assumed to be parallel with either 1-3 plane or 2-3 plane. Figure 8-11 demonstrating one such result in which the amplitude of sine curve is assumed along the 1-3 plane. Lines or curves represented by different colours are defining the variation in the wave frequency depicting the effect of CNT waviness on the elastic properties of PMNC namely C_{11}^{pmnc} , C_{22}^{pmnc} , C_{33}^{pmnc} ,and C_{23}^{pmnc} . It is seen from the figures that the enhancement of the wave frequency leads to the enhancement of the elastic stiffness with respect to the fiber volume fraction when the CNTs are oriented in 1-3 plane and hence, the elastic property C_{11}^{pmnc} showed an increasing nature of properties with increase in amplitude of waviness while C_{22}^{pmnc} , C_{33}^{pmnc} ,and C_{23}^{pmnc} showed in Figs. 9-11 display an opposite trend. This may be attributed to the fact that the transverse isotropy nature of the PMNC with axis 1 in the direction of the CNTs longitudinally becomes the axis of symmetry and the planes 2 and 2 passing through them will certainly be the plane of symmetry and hence the properties so enhancement in stiffness. While, the same shows the opposite trend since the orientation of CNTs differ and hence the decrement in the direction transverse to either

dire 2 or direction 3.

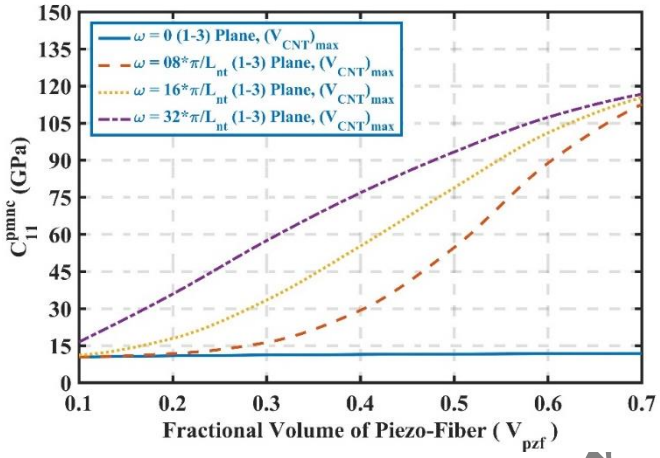

Fig. 8: Effective elastic property of PMNC (C_{11}^{pmnc}) with CNTs oriented along 1-3 plane.

It should also be noted that since the amplitude of the wave or curvature attained by the nanotube is considered along the longitudinal direction i.e. 1-3 direction, the longitudinal elastic property enhances as compared to that of straight nanotube. Since, axis-1 is considered as the axis of transverse isotropy, the results obtained for 2 and 3 directions are identical and hence for the sake of brevity the same has not been displayed here.

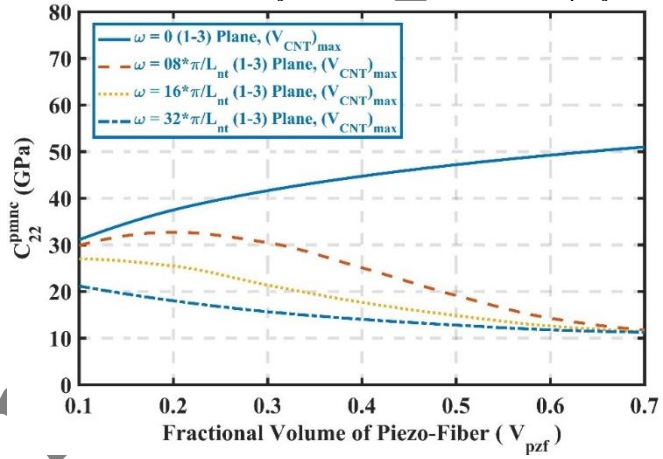

Fig 9: Effective elastic property of PMNC (C_{22}^{pmnc}) with CNTs oriented along 1-3 plane.

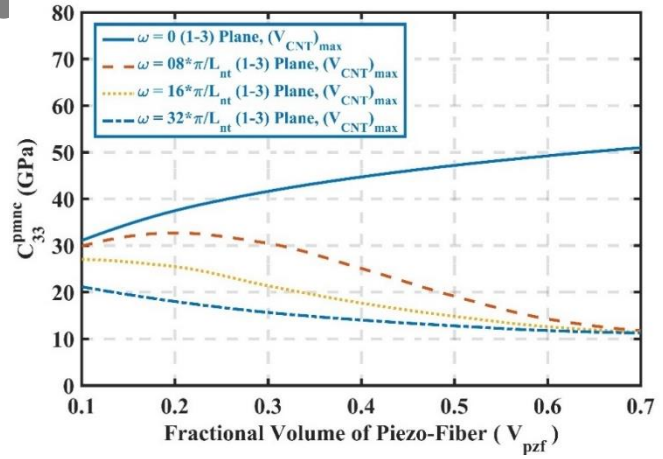

Fig 10: Effective elastic property of PMNC (C_{33}^{pmnc}) with CNTs oriented along 1-3 plane.

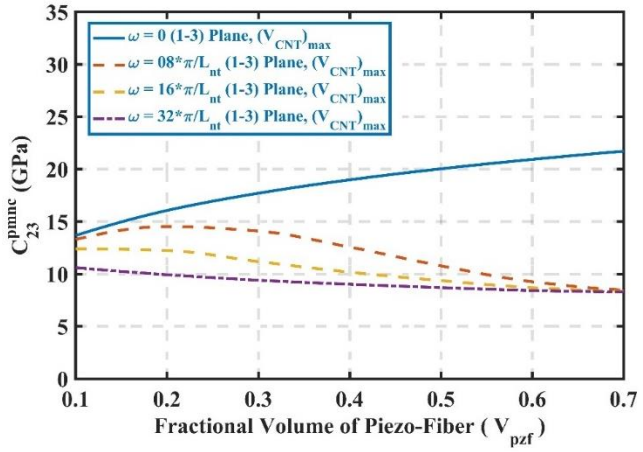

Fig 11: Effective elastic property of PMNC (C_{23}^{pmnc}) with CNTs oriented along 1-3 plane.

Having obtained the elastic coefficient of PMNC the results for the effective elastic properties of piezo fuzzy fiber (PFF) not shown here for brevity sake have been obtained. Taking the micromechanical MOC approach forward, the end effective elastic constants of the short piezo fuzzy fiber reinforced composite (SPFFRC) are displayed in figures 12-16. The results show a similar trend with those of results displayed earlier in Figs. 8-11 which concludes that when the amplitude of the wavy curvature attained by the CNT is along the fiber axis, it enhances the properties associated with that direction only while diminishing the properties transverse to the fiber direction. The reason for this behaviour may be attributed to the fact that the PFF orientation direction remains the axis of transverse isotropy and any plane containing the axis 1 will have enhance properties and hence the enhancement in the properties is seen when the CNTs are oriented in 1-3 plane.

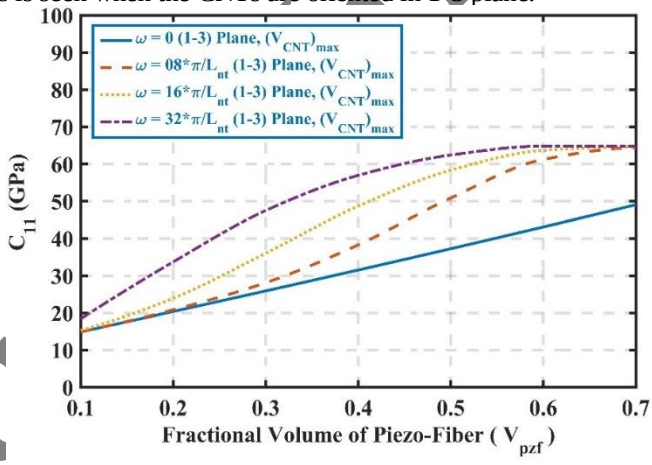

Fig 12: Effective elastic property of SPFFRC (C_{11}) with CNTs oriented along 1-3 plane.

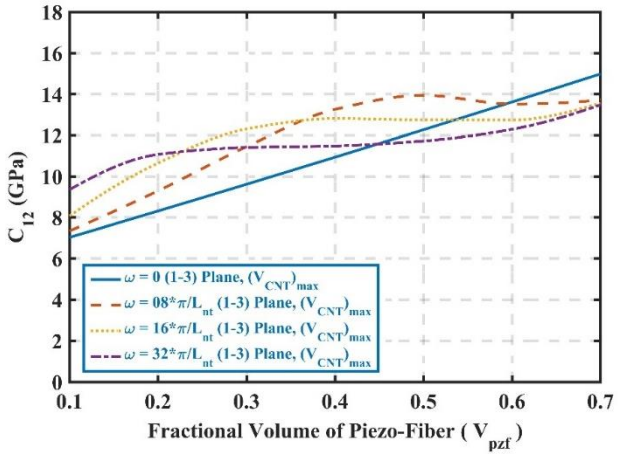

Fig 13: Effective elastic property of SPFFRC (C_{12}) with CNTs oriented along 1-3 plane.

The present work is more focussed on developing the smartness adding materials for attenuation, hence, the effect of CNTs on the piezoelectric properties is an important issue the section forward is dealt with the estimation of the piezoelectric coefficients and their variation with the wave frequency of the CNTs.

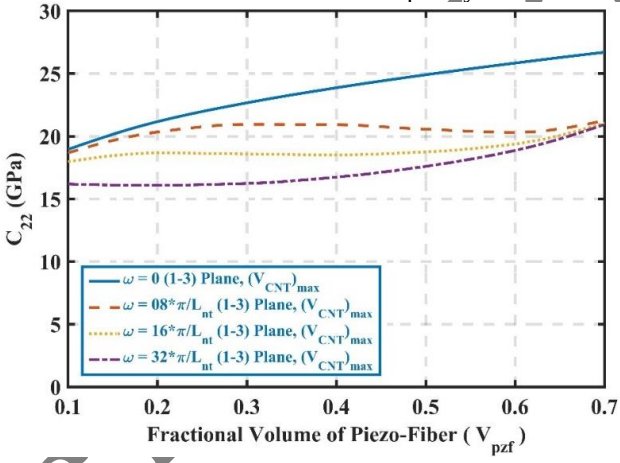

Fig 14: Effective elastic property of SPFFRC (C_{22}) with CNTs oriented along 1-3 plane.

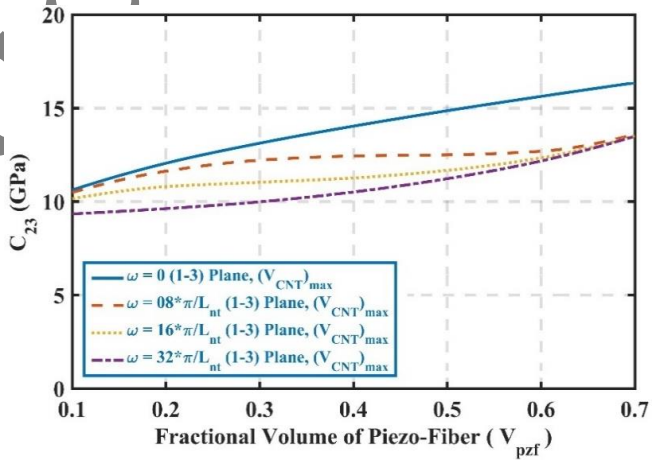

Fig 15: Effective elastic property of SPFFRC (C_{23}) with CNTs oriented along 1-3 plane.

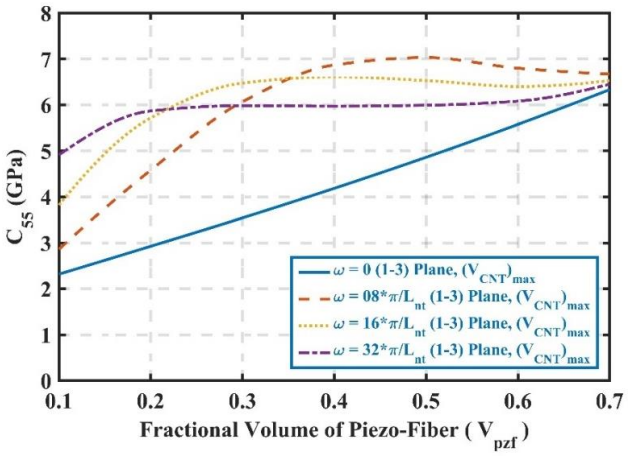

Fig 16: Effective elastic property of SPFFRC (C_{55}) with CNTs oriented along 1-3 plane.

Figures 17 and 18 display the piezo electric properties e_{31}^{pff} and e_{33}^{pff} of piezo fuzzy fiber (PFF) while figures 19 and 20 display the overall piezoelectric properties (e_{31} and e_{33}) of short piezo fuzzy fiber reinforced composite (SPFFRCs) for different waviness of the CNTs. From the Figs. 16 and 17 it can be observed that the piezo electric coefficient e_{31}^{pff} has improvement in absolute value with the increase of wave frequency of CNT while the coefficient e_{33}^{pff} showed as declining trend with increase of waviness of CNTs. However, from the Figs. 18 and 19 it can be seen that the overall piezo electric coefficient e_{31} has no or negligible effect of waviness of CNT but the piezo electric coefficient e_{33} showed a marginal decrease with increase in the waviness of CNTs. Thus, for applicability of the present SPFFRC as material for smart structure, the dominant elastic property shows an increase in value with increase in waviness of CNTs while the piezoelectric coefficients showed a marginal decreasing trend with increase in waviness of CNTs. However, the waviness of CNTs is inevitable and hence it is suggested to consider SPFFRC with wavy CNTs over straight ones for possible application in smartness adding layer of a smart structure.

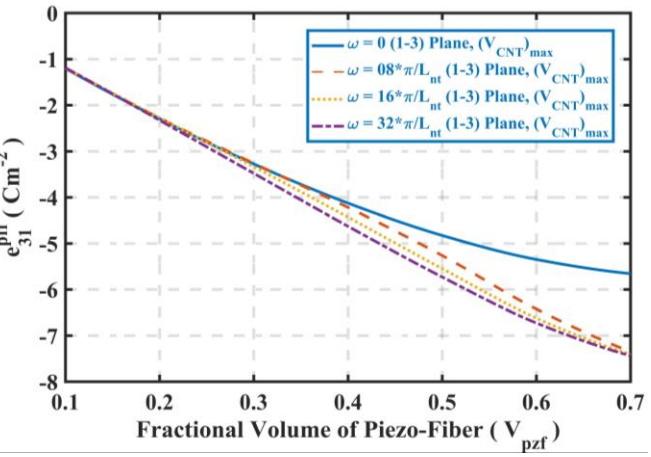

Fig 17: Effective Piezoelectric Coefficient e_{31}^{pff} of PFF with CNTs oriented along 1-3 plane.

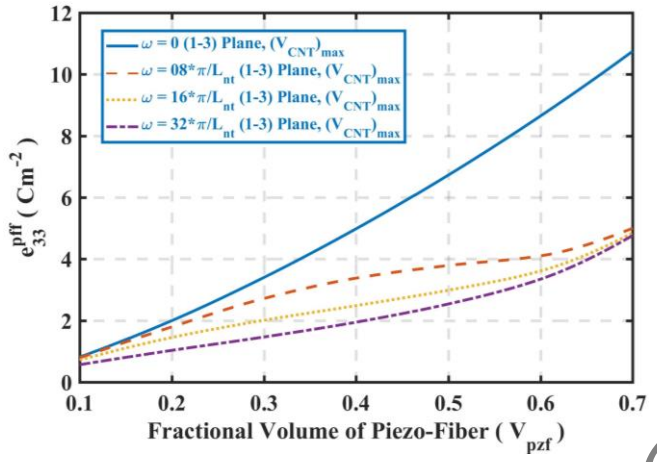

Fig 18: Effective Piezoelectric Coefficient e_{33}^{pff} of PFF with CNTs oriented along 1-3 plane.

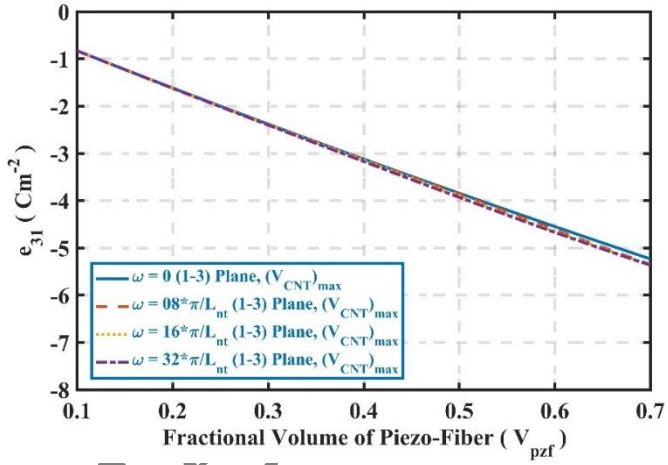

Fig 19: Effective Piezoelectric Coefficient e_{31} of the overall SPFFRC with CNTs oriented along 1-3 plane.

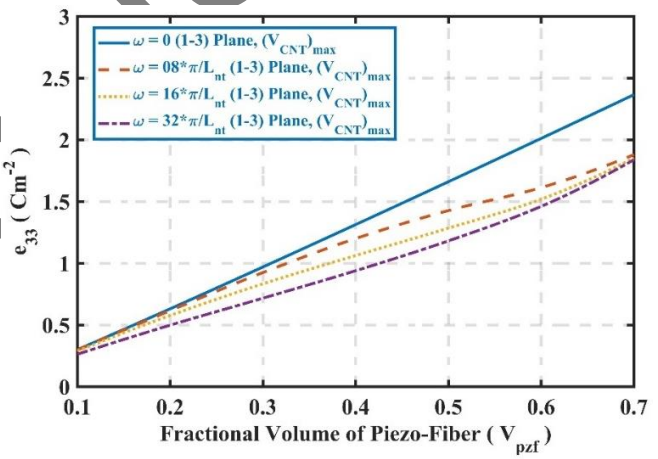

Fig 20: Effective Piezoelectric Coefficient e_{33} of the overall SPFFRC with CNTs oriented along 1-3 plane.

Having observed the effect of waviness of CNTs on overall elastic and piezo electric properties of SPFFRC when the CNTs are aligned in 1-3, the next step is to observe the effect of orientation of CNTs along 2-3 plane on the overall properties of SPFFRCs. The methods described in the earlier sections have been utilized to derive the constitutive elastic coefficient matrix and the piezoelectric coefficient matrix and the results are displaying the following sections. Figures 20 – 22 display the effective elastic properties of PMNCs when the CNTs are oriented along 2-3 directions while the Figs. 24 – 28 display the overall effective elastic and piezo electric coefficient of SPFFRCs when the CNTs are oriented in 2-3 plane.

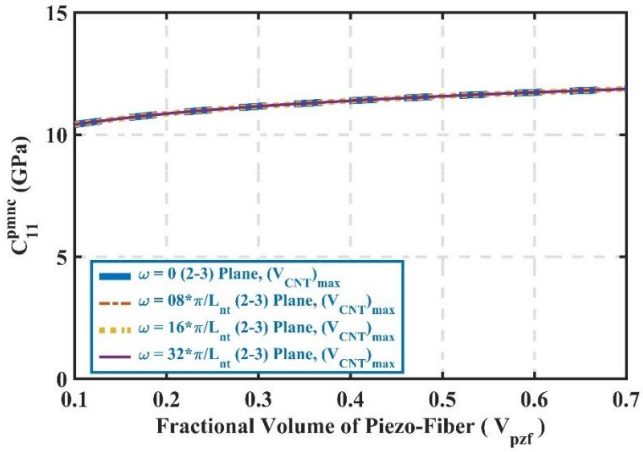

Fig 21: Effective elastic property of PMNC (C_{11}^{pmnc}) with CNTs oriented along 2-3 plane.

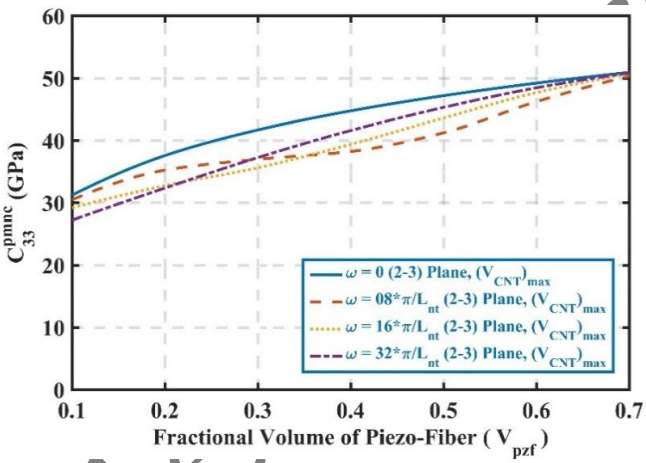

Fig 22: Effective elastic property of PMNC (C_{33}^{pmnc}) with CNTS oriented along 2-3 plane.

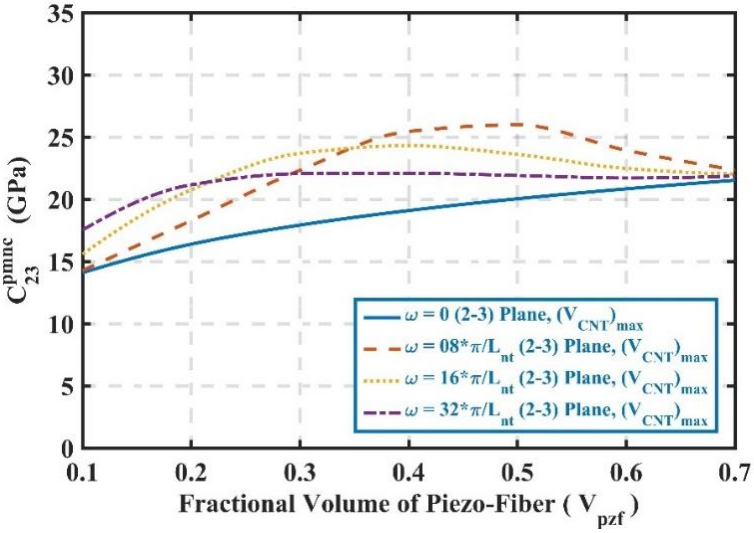

Fig 23: Effective elastic property of PMNC (C_{23}^{pmnc}) with CNTs oriented along 2-3 plane.

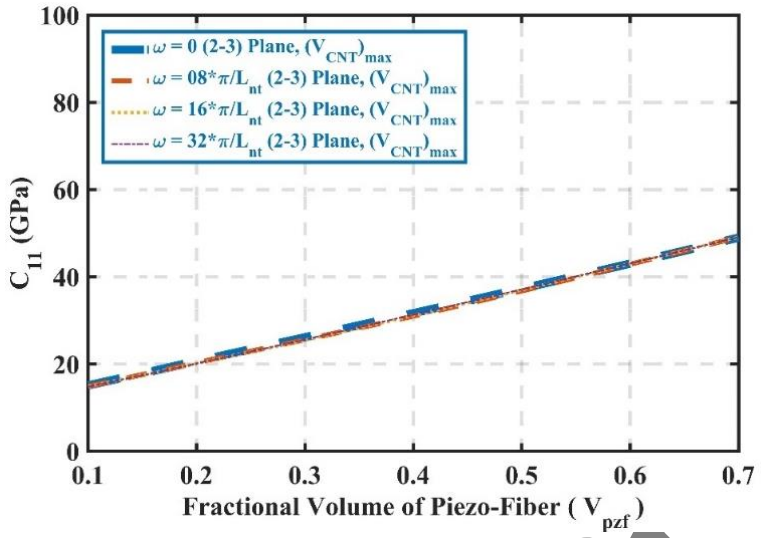

Fig 24: Overall effective elastic property of SPFFRC (C_{11}) with CNTs oriented along 2-3 plane.

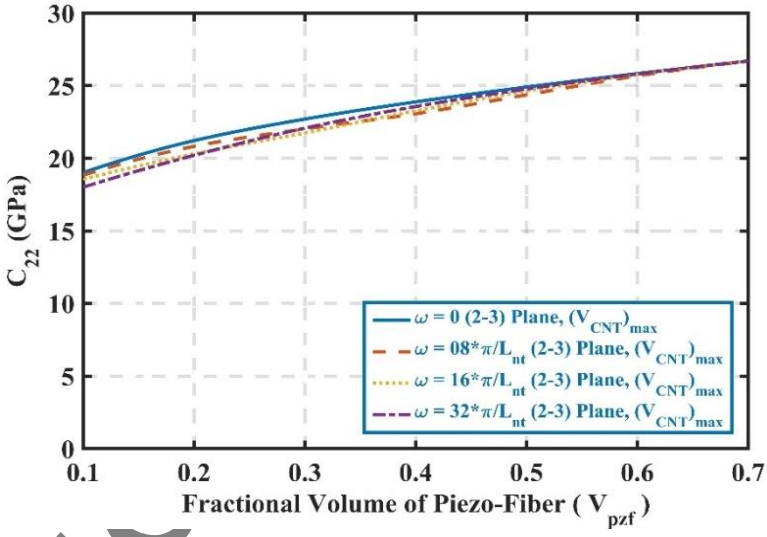

Fig 25: Overall effective elastic property of SPFFRC (C_{22}) with CNTs oriented along 2-3 plane.

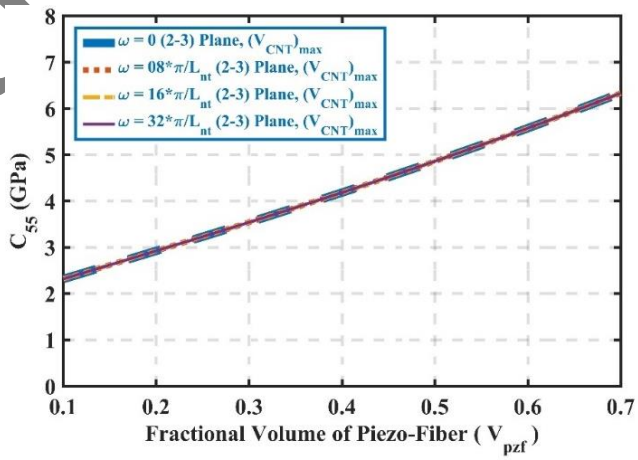

Fig 26: Overall effective elastic property of SPFFRC (C_{55}) with CNTs oriented along 2-3 plane.

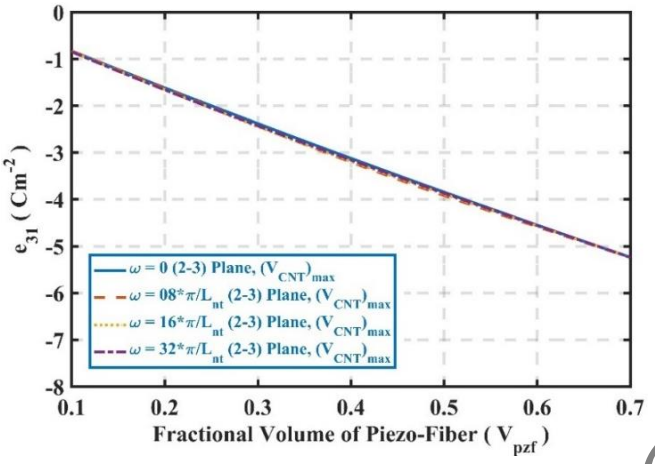

Fig 27: Effective Piezoelectric Coefficient e_{31} of the overall SPFFRC with CNTs oriented along 2-3 plane.

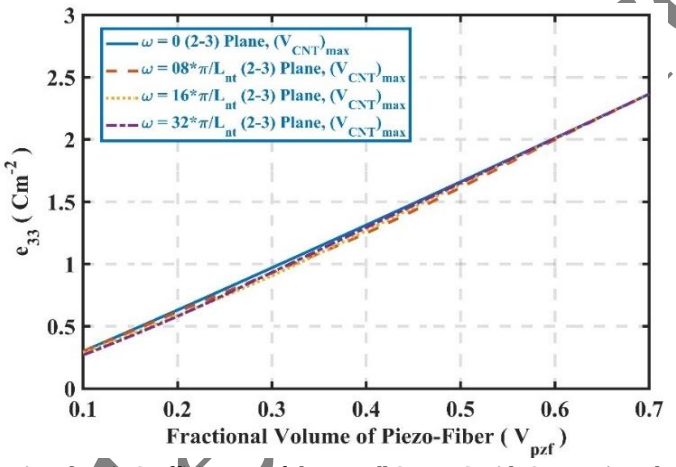

Fig 28: Effective Piezoelectric Coefficient e_{33} of the overall SPFFRC with CNTs oriented along 2-3 plane.

From the figs. 22-23 it can be observed the waviness of CNTs has considerable effect on the properties of PMNC however, the same has no or negligible effect on the overall effective elastic and piezoelectric properties of SPFFRCs for the CNTs orientation along 2-3 plane. This may be attributed to the fact that when the direction of CNTs and the direction of the axis of the base fiber are transverse to each other, the properties get enhanced while the directions transverse to it shows negligible increase in the properties thus corroborating with the fact that the CNTs enhance the properties in transverse directions. Figures 29 to 31 shows the comparisons between the effective properties obtained by MOC approach, and the MT method. Longitudinal property $\boldsymbol{C_{11}}$ displayed in Fig. 29 show little or no deviation between the values obtained by both the MOC and MT approach for lower values of the fiber volume fraction however, of values between those obtained from MOC and MT method start to marginally deviate with increase in the fiber volume fraction.

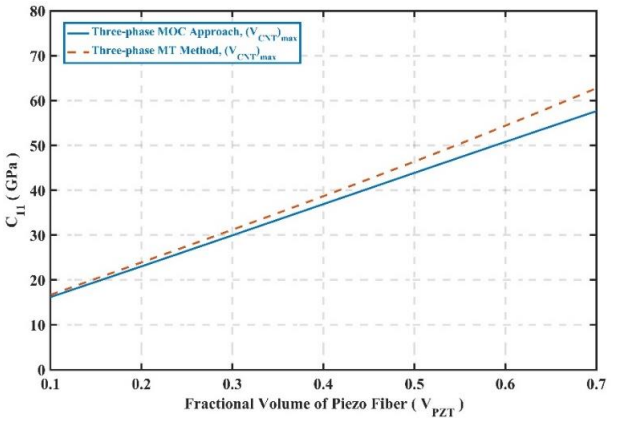

Fig 29: Comparison of effective property C_{11} estimated using MOC approach and MT method.

Figure 30 illustrates the transverse property C_{22} generated using MOC approach is observed with an overestimated magnitude as compared to the estimated value obtained using MT method. The shear property C_{55} illustrated in figure 31 shows that the values estimated using MOC approach is underestimated when compared to those values obtained using MT method. Similar over estimation and under estimation of the properties using MOC approach and MT method were observed by Kundalwal and Ray [29] during their study on short fuzzy fiber reinforced composite thus corroborating the fact that the present micromechanical modelling using MOC and MT method is consistent with the literature. The reason for this behavior although not found in the literature may be understood with the inclusion of fiber cross-section as a square or rectangular and not cirular in deriving the elements of eshelby tensor of the MT method.

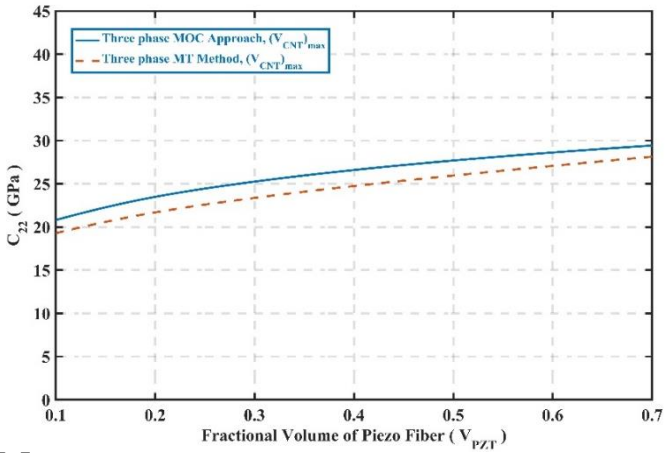

Fig 30: Comparison of effective property C_{22} estimated using MOC approach and MT method.

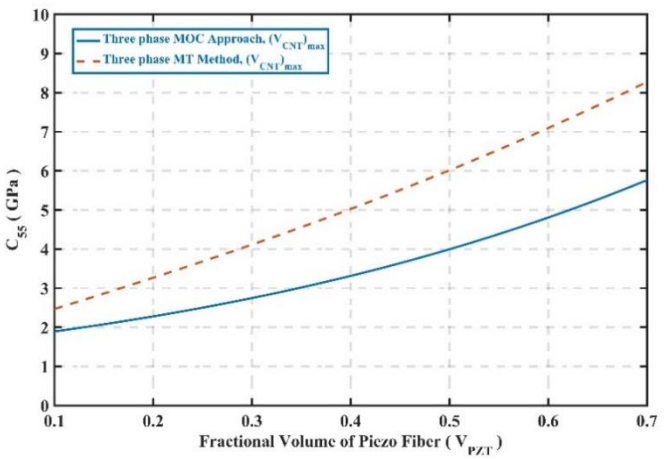

Fig 31: Comparison of effective property C_{55} estimated using MOC approach and MT method.

6. Conclusions:

The present work is focussed on development of micromechanical based method of cells (MOC) model for predicting the effective elastic and piezoelectric properties of short piezo fuzzy fiber reinforced composite (SPFFRC) and the following conclusions are drawn from the present study:

- The validation of the present modelling technique is carried out by modelling similar works existing in the open literature and the result of validations are found to be in good agreement with one another.
- Having validated the present MOC model, the model has been used to estimate the elastic and piezoelectric properties of SPFFRCs when the CNTs are aligned in 1-3, and 2-3 planes, respectively. Also, the waviness being inherent characteristics to the CNTs has also been considered and the effective properties variation with different wave frequencies have been considered for producing the numerical results.
- The results of effective elastic properties of polymer matrix nanocomposite (PMNC) and the final effective properties of short piezo fuzzy fiber reinforced composite (SPFFRC) showed a similar trend when the CNTs are aligned in 1-3 direction while for the CNT orientation in 2-3 plane, the CNT waviness showed significant effect on properties of PMNC but the orientation is found have no significance on over properties of SPFFRCs.
- Also, the wavy CNTs have shown better elastic properties while the straight CNTs have shown better piezoelectric properties however, waviness being inherent characteristic to the CNTs, it is observed that when such SPFFRCs are used as materials for actuator in smart structures, the choice should be such that the overall attenuating effect of these materials is larger compared to exiting conventional piezoelectric composites.
- In order to further corroborate the present model, the results obtained by present MOC approach have been compared with the analytical Mori-Tanaka (MT) method.
- The results showed that few properties are over estimated and few of them have been underestimated which seems to have been the repeated trend observed in the works of earlier researchers [29] thus corroborating the present method of MOC approach for estimation of overall properties of SPFFRCs.

Acknowledgements

The authors acknowledge all the people who are associated with us directly or indirectly in carrying out the research work and making this study possible.

References

[1] M. Ray, A. Faye, S. Patra, R. Bhattacharyya, Theoretical and experimental investigations on the active structural–acoustic control of a thin plate using a vertically reinforced 1-3 piezoelectric composite, *Smart Materials and Structures*, Vol. 18, No. 1, pp. 015012, 2008.

[2] M. Ray, A. Pradhan, On the use of vertically reinforced 1-3 piezoelectric composites for hybrid damping of laminated composite plates, *Mechanics of Advanced Materials and Structures*, Vol. 14, No. 4, pp. 245-261, 2007.

[3] J. W. Sohn, S.-B. Choi, C.-H. Lee, Active vibration control of smart hull structure using piezoelectric composite actuators, *Smart materials and structures*, Vol. 18, No. 7, pp. 074004, 2009.

[4] W. A. Smith, B. A. Auld, Modeling 1-3 composite piezoelectrics: thickness-mode oscillations, *IEEE transactions on ultrasonics, ferroelectrics, and frequency control*, Vol. 38, No. 1, pp. 40-47, 1991.

[5] N. Mallik, M. Ray, Effective coefficients of piezoelectric fiber-reinforced composites, *AIAA journal*, Vol. 41, No. 4, pp. 704-710, 2003.

[6] S. Iijima, Helical microtubules of graphitic carbon, *nature*, Vol. 354, No. 6348, pp. 56-58, 1991.

[7] M. J. Treacy, T. W. Ebbesen, J. M. Gibson, Exceptionally high Young's modulus observed for individual carbon nanotubes, *nature*, Vol. 381, No. 6584, pp. 678-680, 1996.

[8] L. Shen, J. Li, Transversely isotropic elastic properties of single-walled carbon nanotubes, *Physical Review B*, Vol. 69, No. 4, pp. 045414, 2004.

[9] H.-C. Cheng, Y.-L. Liu, Y.-C. Hsu, W.-H. Chen, Atomistic-continuum modeling for mechanical properties of single-walled carbon nanotubes, *International Journal of Solids and Structures*, Vol. 46, No. 7-8, pp. 1695-1704, 2009.

[10] E. T. Thostenson, T.-W. Chou, On the elastic properties of carbon nanotube-based composites: modelling and characterization, *Journal of Physics D: Applied Physics*, Vol. 36, No. 5, pp. 573, 2003.

[11] M. Griebel, J. Hamaekers, Molecular dynamics simulations of the elastic moduli of polymer–carbon nanotube composites, *Computer methods in applied mechanics and engineering*, Vol. 193, No. 17-20, pp. 1773-1788, 2004.

[12] G. Odegard, T. Clancy, T. Gates, Modeling of the mechanical properties of nanoparticle/polymer composites, *Polymer*, Vol. 46, pp. 553-562, 2005.

[13] G. D. Seidel, D. C. Lagoudas, Micromechanical analysis of the effective elastic properties of carbon nanotube reinforced composites, *Mechanics of materials*, Vol. 38, No. 8-10, pp. 884-907, 2006.

[14] Y. S. Song, J. R. Youn, Modeling of effective elastic properties for polymer based carbon nanotube composites, *Polymer*, Vol. 47, No. 5, pp. 1741-1748, 2006.

[15] B. Jiang, C. Liu, C. Zhang, R. Liang, B. Wang, Maximum nanotube volume fraction and its effect on overall elastic properties of nanotube-reinforced composites, *Composites Part B: Engineering*, Vol. 40, No. 3, pp. 212-217, 2009.

[16] M. Ayatollahi, S. Shadlou, M. Shokrieh, Multiscale modeling for mechanical properties of carbon nanotube reinforced nanocomposites subjected to different types of loading, *Composite Structures*, Vol. 93, No. 9, pp. 2250-2259, 2011.

[17] F. Fisher, R. Bradshaw, L. Brinson, Effects of nanotube waviness on the modulus of nanotube-reinforced polymers, *Applied Physics Letters*, Vol. 80, No. 24, pp. 4647-4649, 2002.

[18] M. Ray, R. Batra, Effective properties of carbon nanotube and piezoelectric fiber reinforced hybrid smart composites, 2009.

[19] C. Bower, W. Zhu, S. Jin, O. Zhou, Plasma-induced alignment of carbon nanotubes, *Applied Physics Letters*, Vol. 77, No. 6, pp. 830-832, 2000.

[20] G. Lanzara, F. Chang, Novel processes to reinforce the piezoelectric actuator interface with carbon nanotubes, in *Proceeding of*, SPIE, pp. 352-361.

[21] R. Mathur, S. Chatterjee, B. Singh, Growth of carbon nanotubes on carbon fibre substrates to produce hybrid/phenolic composites with improved mechanical properties, *Composites Science and Technology*, Vol. 68, No. 7-8, pp. 1608-1615, 2008.

[22] G. Lanzara, F. Chang, Design and characterization of a carbon-nanotube-reinforced adhesive coating for piezoelectric ceramic discs, *Smart Materials and Structures*, Vol. 18, No. 12, pp. 125001, 2009.

[23] E. J. Garcia, B. L. Wardle, A. J. Hart, N. Yamamoto, Fabrication and multifunctional properties of a hybrid laminate with aligned carbon nanotubes grown in situ, *Composites Science and Technology*, Vol. 68, No. 9, pp. 2034-2041, 2008.

[24] J.-L. Tsai, S.-H. Tzeng, Y.-T. Chiu, Characterizing elastic properties of carbon nanotubes/polyimide nanocomposites using multi-scale simulation, *Composites Part B: Engineering*, Vol. 41, No. 1, pp. 106-115, 2010.

[25] Q. Zhang, W. Qian, R. Xiang, Z. Yang, G. Luo, Y. Wang, F. Wei, In situ growth of carbon nanotubes on inorganic fibers with different surface properties, *Materials Chemistry and Physics*, Vol. 107, No. 2-3, pp. 317-321, 2008.

[26] A. Alian, S. Kundalwal, S. Meguid, Interfacial and mechanical properties of epoxy nanocomposites using different multiscale modeling schemes, *Composite Structures*, Vol. 131, pp. 545-555, 2015.

[27] S. Kundalwal, M. Ray, Micromechanical analysis of fuzzy fiber reinforced composites, *International Journal of Mechanics and Materials in Design*, Vol. 7, pp. 149-166, 2011.

[28] S. Kundalwal, M. Ray, Effective properties of a novel continuous fuzzy-fiber reinforced composite using the method of cells and the finite element method, *European Journal of Mechanics-A/Solids*, Vol. 36, pp. 191-203, 2012.

[29] S. Kundalwal, M. Ray, Effective properties of a novel composite reinforced with short carbon fibers and radially aligned carbon nanotubes, *Mechanics of Materials*, Vol. 53, pp. 47-60, 2012.

[30] S. Kundalwal, M. Ray, Effect of carbon nanotube waviness on the effective thermoelastic properties of a novel continuous fuzzy fiber reinforced composite, *Composites Part B: Engineering*, Vol. 57, pp. 199-209, 2014.

[31] S. Kundalwal, M. Ray, Effect of carbon nanotube waviness on the elastic properties of the fuzzy fiber reinforced composites, *Journal of Applied Mechanics,* Vol. 80, No. 2, pp. 021010, 2013.

[32] M. Mohammadi, M. Goodarzi, M. Ghayour, A. Farajpour, Influence of in-plane pre-load on the vibration frequency of circular graphene sheet via nonlocal continuum theory, *Composites Part B: Engineering,* Vol. 51, pp. 121-129, 2013.

[33] M. Mohammadi, A. Farajpour, A. Moradi, M. Ghayour, Shear buckling of orthotropic rectangular graphene sheet embedded in an elastic medium in thermal environment, *Composites Part B: Engineering,* Vol. 56, pp. 629-637, 2014.

[34] M. Mohammadi, A. Farajpour, M. Goodarzi, Numerical study of the effect of shear in-plane load on the vibration analysis of graphene sheet embedded in an elastic medium, *Computational Materials Science,* Vol. 82, pp. 510-520, 2014.

[35] M. Mohammadi, A. Farajpour, M. Goodarzi, F. Dinari, Thermo-mechanical vibration analysis of annular and circular graphene sheet embedded in an elastic medium, *Latin American Journal of Solids and Structures,* Vol. 11, pp. 659-682, 2014.

[36] M. Mohammadi, A. Moradi, M. Ghayour, A. Farajpour, Exact solution for thermo-mechanical vibration of orthotropic mono-layer graphene sheet embedded in an elastic medium, *Latin American Journal of Solids and Structures,* Vol. 11, pp. 437-458, 2014.

[37] A. Ghorbanpour Arani, E. Haghparast, A. Ghorbanpour Arani, Size-dependent vibration of double-bonded carbon nanotube-reinforced composite microtubes conveying fluid under longitudinal magnetic field, *Polymer Composites,* Vol. 37, No. 5, pp. 1375-1383, 2014.

[38] A. Ghorbanpour Arani, M. Jamali, A. Ghorbanpour-Arani, R. Kolahchi, M. Mosayyebi, Electro-magneto wave propagation analysis of viscoelastic sandwich nanoplates considering surface effects, *Proceedings of the Institution of Mechanical Engineers, Part C: Journal of Mechanical Engineering Science,* Vol. 231, No. 2, pp. 387-403, 2015.

[39] A. Ghorbanpour-Arani, A. Rastgoo, M. Sharafi, R. Kolahchi, A. Ghorbanpour Arani, Nonlocal viscoelasticity based vibration of double viscoelastic piezoelectric nanobeam systems, *Meccanica,* Vol. 51, pp. 25-40, 2015.

[40] A. Ghorbanpour-Arani, A. Rastgoo, A. Hafizi Bidgoli, R. Kolahchi, A. Ghorbanpour Arani, Wave propagation of coupled double-DWBNNTs conveying fluid-systems using different nonlocal surface piezoelasticity theories, *Mechanics of Advanced Materials and Structures,* Vol. 24, No. 14, pp. 1159-1179, 2016.

[41] A. Ghorbanpour-Arani, M. Abdollahian, A. Ghorbanpour Arani, Nonlinear dynamic analysis of temperature-dependent functionally graded magnetostrictive sandwich nanobeams using different beam theories, *Journal of the Brazilian Society of Mechanical Sciences and Engineering,* Vol. 42, pp. 1-20, 2020.

[42] E. Haghparast, A. Ghorbanpour-Arani, A. G. Arani, Effect of fluid–structure interaction on vibration of moving sandwich plate with Balsa wood core and nanocomposite face sheets, *International Journal of Applied Mechanics,* Vol. 12, No. 07, pp. 2050078, 2020.

[43] M. Mohammadi, A. Farajpour, A. Moradi, M. Hosseini, Vibration analysis of the rotating multilayer piezoelectric Timoshenko nanobeam, *Engineering Analysis with Boundary Elements,* Vol. 145, pp. 117-131, 2022.

[44] A. A. Ghorbanpour-Arani, Z. Khoddami Maraghi, A. Ghorbanpour Arani, The frequency response of intelligent composite sandwich plate under biaxial in-plane forces, *Journal of Solid Mechanics,* Vol. 15, No. 1, pp. 1-18, 2023.

[45] M. Mohammadi, A. Farajpour, A. Rastgoo, Coriolis effects on the thermo-mechanical vibration analysis of the rotating multilayer piezoelectric nanobeam, *Acta Mechanica,* Vol. 234, No. 2, pp. 751-774, 2023.

[46] M. Mohammadi, M. Safarabadi, A. Rastgoo, A. Farajpour, Hygro-mechanical vibration analysis of a rotating viscoelastic nanobeam embedded in a visco-Pasternak elastic medium and in a nonlinear thermal environment, *Acta Mechanica,* Vol. 227, pp. 2207-2232, 2016.

[47] P. Wan, M. Al-Furjan, R. Kolahchi, L. Shan, Application of DQHFEM for free and forced vibration, energy absorption, and post-buckling analysis of a hybrid nanocomposite viscoelastic rhombic plate assuming CNTs' waviness and agglomeration, *Mechanical Systems and Signal Processing,* Vol. 189, pp. 110064, 2023.

[48] M. Al-Furjan, S. Fan, L. Shan, A. Farrokhian, X. Shen, R. Kolahchi, Wave propagation analysis of micro air vehicle wings with honeycomb core covered by porous FGM and nanocomposite magnetostrictive layers, *Waves in Random and Complex Media*, pp. 1-30, 2023.

[49] L. Shan, C. Tan, X. Shen, S. Ramesh, M. Zarei, R. Kolahchi, M. Hajmohammad, The effects of nano-additives on the mechanical, impact, vibration, and buckling/post-buckling properties of composites: A review, *Journal of Materials Research and Technology*, 2023.

[50] C. Chu, L. Shan, M. Al-Furjan, A. Farrokhian, R. Kolahchi, Energy absorption, free and forced vibrations of flexoelectric nanocomposite magnetostrictive sandwich nanoplates with single sinusoidal edge on the frictional torsional viscoelastic medium, *Archives of Civil and Mechanical Engineering*, Vol. 23, No. 4, pp. 223, 2023.

[51] C. Chu, M. Al-Furjan, R. Kolahchi, Energy harvesting and dynamic response of SMA nano conical panels with nanocomposite piezoelectric patch under moving load, *Engineering Structures*, Vol. 292, pp. 116538, 2023.

[52] P. Wan, M. Al-Furjan, R. Kolahchi, Nonlinear flutter response and reliability of supersonic smart hybrid nanocomposite rupture trapezoidal plates subjected to yawed flow using DQHFEM, *Aerospace Science and Technology*, Vol. 145, pp. 108862, 2024.

[53] S. Dhala, M. Ray, Micromechanics of piezoelectric fuzzy fiber-reinforced composite, *Mechanics of Materials*, Vol. 81, pp. 1-17, 2015.

[54] J. Aboudi, Micromechanical analysis of composites by the method of cells, 1989.

[55] T. Mori, K. Tanaka, Average stress in matrix and average elastic energy of materials with misfitting inclusions, *Acta metallurgica*, Vol. 21, No. 5, pp. 571-574, 1973.

[56] Y. Qiu, G. Weng, On the application of Mori-Tanaka's theory involving transversely isotropic spheroidal inclusions, *International Journal of Engineering Science*, Vol. 28, No. 11, pp. 1121-1137, 1990.

Appendix

For the evaluation of the maximum volume fraction of the carbon nanotube in the overall nanocomposite, the representative volume element drawn of the piezoelectric fiber composite can be taken into consideration. Here, the RVE is thought to be shaped like an equilateral triangle. The volume might therefore be shown as

$$V^{spffrc} = \frac{\sqrt{3}}{4} D_{pff}^2 L_{fiber} \tag{A1}$$

Where, $D_{pff}^2 = 2R$ is the diameter of the piezoelectric fuzzy fiber. The volume of the piezo fiber is given by

$$V^{pzf} = \frac{\pi}{8} d_{fiber}^2 L_{fiber} \tag{A2}$$

Where, $d_{fiber} = 2a$. So, the volume fraction of the fiber in nanocomposite could be derived here as

$$V_{pzf} = \frac{V^{pzf}}{V^{spffrc}} = \frac{\pi}{2\sqrt{3}} \frac{1}{\eta B_r^2} \tag{A3}$$

Where, $\eta = L/L_f$ and $B_r = D_{pff}/d_{fiber}$.

The volume percentage of the fiber in relation to the piezoelectric fuzzy fiber (PFF), can also be estimated using eq. (A3). Following could be drawn from the same.

$$\overline{V}_{pzf} = \frac{\frac{\pi}{8} d_{fiber}^2 L_{fiber}}{\frac{\pi}{8} D_b^2 L_{fiber}} = \frac{1}{B_b^2} \tag{A4}$$

Where, $D_b = 2b$ and $B_b = D_b/d_{fiber}$

The carbon nanotubes are supposed to grow radially on the circumferential surface of the Piezo fiber, which is the innovative constructional aspect taken into consideration here. Thus, maximum number of this aligned radial nanotubes could be estimated as

$$\left(N_{cnt}\right)_{\max} = \frac{\pi d_{fiber} L_{fiber}}{2\left(d_{nt} + 1.7\right)^2} \tag{A5}$$

Now the Volume of the radial nanotube is given by

$$V^{cnt} = \frac{\pi}{4} d_{nt}^2 L_n \left(N_{cnt}\right)_{\max} \tag{A6}$$

Where, $L_n = R - a$.

The following derivation could be used to estimate the maximum volume fraction of the nanotube in relation to the nanocomposite using the equations above.

$$\left(V_{cnt}\right)_{\max} = \frac{V^{cnt}}{V^{spffrc}} = \frac{\pi d_{nt}^2}{2\left(d_{nt} + 1.7\right)^2}\left(B_b - 1\right)V_{pzf} \tag{A7}$$

The value of the maximum volume fraction of the carbon nanotube with respect to the polymer matrix nanocomposite will then be determined using equation (A7).

$$\left(V_{nt}\right)_{\max} = \frac{V^{cnt}}{V^{pmnc}} = \frac{\left(v_{cnt}\right)_{\max}}{\left(B_b^2 - 1\right)V_{pzf}} \tag{A8}$$

Additionally, the interphase's maximum volume fraction in relation to the polymer matrix nanocomposite is calculated.

$$\left(v_i\right)_{\max} = \frac{V^i}{V^{pmnc}} = \frac{\left(d_i^2 - d_n^2\right)}{d_n^2}\left(V_{nt}\right)_{\max} \tag{A9}$$